Achieving Per-Flow Satisfaction with Multi-Path D2D*

Edgar Arribas[a,b,c,*], Vincenzo Mancuso[a,c]

[a] *IMDEA Networks Institute*
[b] *Universidad Carlos III de Madrid*
[c] *Avda. del Mar Mediterráneo, 22, Leganés (Madrid)*

Abstract

Device-to-Device (D2D) communication allows for users placed in a cell to establish direct connections with each other using several connection modes. In this paper, we propose *Multi-Path D2D (MPD2D)*, a mathematical optimization framework that accounts for the availability of D2D modes under the requirements dictated by a process of flow requests. MPD2D selects the combination of cellular and D2D links that boosts network performance as much as possible. We consider *Underlay* and *Overlay* as *Inband* D2D modes reusing cellular frequencies with scheduled resources and the *Outband* D2D mode exploiting WLAN frequencies and the 802.11 random access scheme to complement cellular resources. We model throughput, energy consumption, interference, and per-flow network requirements, so to define a network utility function that accounts for throughput and power efficiency. Moreover, we formulate a user satisfaction metric that accounts for the history of users within the cell. Integrating such a metric in a throughput optimization problem is lightweight yet very effective to drive towards almost complete fairness. Our optimization scheme is formulated as a Binary Non-Linear Program, which results in higher throughput performance in comparison to other state-of-the-art solutions we have tested. Finally, we propose two effective heuristics, whose performance is near-optimal, whereas their complexity scales polynomially with the number of users.

Keywords: Device-to-Device, D2D Networks, Optimization, *Inband* D2D, *Outband* D2D.

1. Introduction

Fast advance in the design of 5G cellular networks has motivated many research works in the recent years [2]. The main research challenges are given by the explosive growth of traffic burden [3], the rise of energy consumption constraints, the unprecedentedly high demand for broadband mobile connectivity and Quality of Service (QoS) [4]. Therefore the appearance of new technologies and system designs is vital to bear such high demand in networks infrastructures [5].

The appealing concept of *Device-to-Device (D2D) Communications* has been proposed in order to improve network performance in sight of the ambitious service optimization goals of 5G networks. D2D

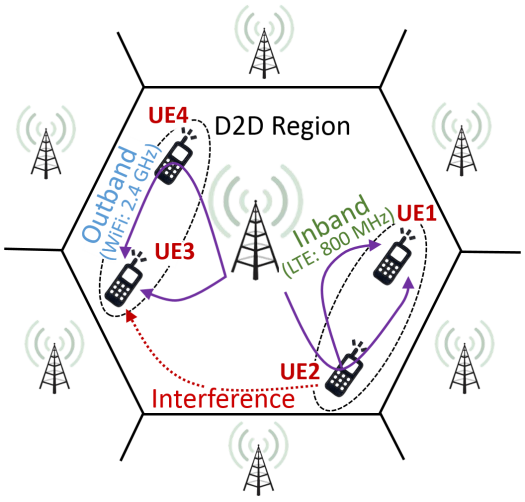

Figure 1: D2D-enabled cellular network.

*A preliminary 7-page version of this manuscript appeared in the proceedings of IEEE WoWMoM 2017 [1].
*Corresponding author.
Email addresses: edgar.arribas@imdea.org (Edgar Arribas), vincenzo.mancuso@imdea.org (Vincenzo Mancuso)

This paper has been accepted for publication in the Journal Ad Hoc Networks on March 27th, 2020. Submitted on Match 15th, 2019.

allows to widen the coverage of cellular networks at lower energy costs through direct links between devices in close range without traversing a base station (BS) or the core of the network [6]. D2D-enabled networking has been an important topic of research during the recent years, due to its promising capabilities to accomplish networks requirements. Both cellular (3GPP) and WLAN (e.g., WiFi) development organizations have produced specifications for D2D, e.g., the eProSe in 3GPP [7] and WiFi Direct [8]; and Android developers now provide support for D2D through the Google Nearby API [9]. Indeed recent research has demonstrated how D2D can be incorporated into cellular networks through WiFi Direct and 3GPP cellular technologies for 4G and 5G [10, 11, 12]. In this paper, we exploit both WLAN and 3GPP cellular technologies in order to maximize throughput and energy efficiency while targeting flow fairness when *Inband Underlay* and *Overlay*, and *Outband* D2D *modes* are enabled. Specifically, we derive an optimization scheme that allows the cellular network to coordinate D2D communications in the network.

Several studies have analyzed *Inband* and *Outband* D2D modes and identified their potential contribution (see, e.g., [13, 14]). More specifically, D2D has been analyzed for what concerns cellular traffic offloading [15], QoS [16] and for what concerns its application to traffic relaying [17]. However, a deep review on D2D literature shows that, despite all struggles in optimizing the use of D2D, there is no D2D mode that clearly fits better than all others to its integration into cellular networks when the system requires the enhancement of traffic offloading and QoS conditions [18].

In order to determine which mode fits the best, in [19] we find one of the few works where multiple D2D modes are enabled and coupled at once, exploiting their benefits and minimizing their drawbacks. Other approaches to relay through D2D are available, which however do not exploit multi-homing of modern devices and multi-path possibilities offered by D2D links, e.g., Group D2D Mode (GMD2D) [20], Underlay MSP [21] and Outband D2D [22]. The one in [19] was the first work that derived a theoretical model for an adaptive multi-mode framework in which *Inband Underlay* and *Overlay*, and *Outband* connection modes are coupled in a cell. However, we find that the framework proposed in [19], *Floating Band D2D*, relies on limiting assumptions for fitting into a real cellular scenario. In the rest of this paper we refer to Floating Band D2D as FBD2D for convenience. We point out that FBD2D does not exploit some key D2D features. For instance, FBD2D neither allows using both LTE (Long Term Evolution) and WiFi at the same time nor embeds flow demand requirements and user satisfaction in the D2D decision making process. Instead, we incorporate more flexibility and the use of concurrent D2D modes in our proposal while accounting for user satisfaction on a per-flow level.

Specifically, in this paper, we propose a theoretical framework to tackle the *mode selection problem (MSP)* for D2D-enabled cellular networks in a *stateful* manner and under fairness constraints computed not just on individual throughputs but rather on network flows. We exploit both cellular and WLAN technologies to maximize throughput and energy efficiency while targeting flow fairness when *Inband Underlay* and *Overlay*, and *Outband* D2D *modes* are enabled. As main contributions, we develop an optimization scheme that adaptively selects in which mode each user equipment (UE) will set links to D2D pairs or to the BS in benefit of a network utility function. Unlike past works, we consider flow demands between D2D neighbors and with the BS, and impose their fulfilment through **multi-path** and **relaying**. Indeed, with our proposal, each UE may use simultaneously both cellular and WLAN interfaces for either transmission or reception, thus obtaining higher throughput rates with respect to using only D2D or only cellular connectivity. Moreover, flows can be served over multiple paths within the cellular network, through D2D paths. To reduce complexity and lessen the negative impact on energy consumption and latency due to multi-hop routing, we limit

the scope of our approach to direct cellular links and two-hop D2D paths. Besides, we derive a stateful *satisfaction metric* which is aware of past users' opportunities and increases chances of connections in close future to UEs that enjoyed less throughput. We summarize the main contributions of this paper:

- We introduce MPD2D, a multi-mode D2D framework designed to address the mode selection problem in cellular networks in order to optimize network performance in terms of energy consumption and network data flows throughput.
- We propose to use multiple paths to deliver network flows by means of two-hop D2D relaying with several MAC interfaces.
- We propose the implementation of a satisfaction metric that accounts for past users' experience and increases the connection opportunities in close future for those users that have experienced less benefits from the network in the past. To this end, we derive the DEMA scheme, which has negligible computational cost and achieves very relevant gains in terms of fairness of users' satisfaction.
- We mathematically formulate a Binary Non-Linear optimization program and reformulate it as an MILP in order to solve it with standard tools.
- We propose two effective heuristics, DIMM and DEMM, that are shown to be close-to-optimal, and that reduce complexity and make the deployment of the framework feasible in real cellular networks.
- We perform extensive simulations in comparison to state-of-the-art proposals to show the high gains that MPD2D reaches in terms of network throughput, user energy consumption, network efficiency and users' satisfaction fairness over time.

In Figure 1 we see how flows are split onto heterogeneous multiple paths to get to their destinations through relaying and/or direct connections. For instance, the figure shows that there is a traffic flow from the BS targeting *UE1*. This traffic follows first a cellular link to *UE2*. Then, *UE2* relays the traffic over two D2D links exploiting *Inband* and *Outband* modes. Also, the traffic from the BS to *UE3* splits over a direct cellular link and a relayed path through *UE4*. *UE4* downloads part of the traffic for *UE3* and forwards the data over *Outband* D2D mode exploiting WLAN resources. Hence, our proposed framework speeds up traffic flow deliveries reducing the effect of network bottlenecks, by means of multiple traffic paths.

We name our D2D scheme *Multi-Path D2D (MPD2D)*, which results in an NP-hard Binary Non-Linear Program, and propose two effective heuristics in order to approximate the optimal solution of the problem. As a result, we observe that the heuristics for solving MPD2D dramatically increase the performance of cellular networks in comparison to several benchmarks. Specifically, we compare our proposal to the following state of the art solutions/proposals explicitly designed for relay networks based on D2D, namely FBD2D [19], Group D2D Mode (GMD2D) [20], Underlay MSP [21] and Outband D2D [22].

This paper updates and extends the content presented in [1] for MPD2D, and includes the following new technical contributions: First, we have added the new Subsection 3.4, to provide deep insights on DEMA, our novel one-step-memory filtering process used to measure the satisfaction of users when finite-duration traffic flows are served in the network. Due to space limitations, we could not provide deep insights on DEMA in [1]. Here we analyze it and

compare DEMA to other approaches and provide three new plots (Figures A.7a, A.7b and A.7c) showing the benefits of DEMA in Appendix A. Second, we have considerably extended the numerical evaluation by testing more scenarios. We have included seven new figures out of fifteen in Section 6, so to provide a deeper performance evaluation of the optimal behavior of MPD2D and proposed heuristics under realistic cellular and D2D technology options, and also with respect to other state-of-the-art proposals. Third, we show in Appendix B how to turn the mathematical optimization framework presented in Subsection 4.3 (which is a Mixed-Integer Non-Linear Optimization Program) into a tractable Mixed-Integer Linear Program, for which it is possible to find optima through efficient algorithms as Branch&Bound.

The rest of the paper is structured as follows. Section 2 provides a state-of-the-art discussion on D2D communications and adaptive D2D networks. Section 3 shows our proposal: MPD2D. Section 4 presents the optimization formulation. Section 5 provides two practical heuristics, while in Section 6 we numerically evaluate and benchmark MPD2D and the heuristics. Section 7 concludes the paper.

2. Background on D2D Networks and Related Work

Coupling D2D technology and cellular networks is not restricted to any wireless technology [6]. A D2D link is a direct connection between two UEs without traversing a BS or the core of the network, thus providing infrastructureless communications. There are main *D2D modes* proposed to set D2D links between UEs. A *D2D mode* specifies through which band devices connect (licensed or unlicensed) and how UEs access the physical resources. Finding the way of setting the proper D2D mode is key in order to optimize a D2D-network under delay, throughput or energy constraints [18]. The 3rd Generation Partnership Project (3GPP) provides on technical reports the technological specifications and needs of *Proximity-based Services (eProSe)* for enabling D2D communications on current cellular networks [7]. 3GPP will enable users to offload and relay traffic, share content, and ensure the D2D network by means of cooperative use of the different D2D connectivity modes.

We present the main D2D modes developed for a D2D-enabled cellular network. We incorporate the *cellular mode* since it is the most common connection mode in a cell.

- Mode 0: **Cellular mode.** Cellular connection between a UE and the BS in either uplink or downlink.
- Mode 1: **Inband Underlay.** D2D connection between two UEs on the licensed band. UEs reuse cellular resources. Spectrum is shared with cellular devices.
- Mode 2: **Inband Overlay.** D2D connection between two UEs on the licensed spectrum over a resource portion dedicated only to this D2D mode. Spectrum is reused only among D2D UEs over this mode.
- Mode 3: **Outband.** D2D connection between two UEs in unlicensed spectrum. Medium access control and interference is not under the control of the BS.

These modes have been widely studied in literature. Researchers have studied crucial matters in current networks, such as spectral efficiency, power efficiency, QoS [16], cellular coverage [23], network offloading [15], etc. Each mode enjoys technological properties and medium access opportunities clearly distinct, which originates a discussion about which D2D mode fits better in a cellular network [18]. In Table 1 we show the main advantages and drawbacks of each D2D mode, which motivates the integration of frameworks as FBD2D [19] or MPD2D, in order to exploit their advantages and reduce the effects of their drawbacks. As these frameworks account for switching from LTE

Table 1: Pros and Cons of each D2D mode

	Advantages	Drawbacks
Mode 1: *Underlay*	Rise of spectral efficiency. Same interface as cellular. SINR control is in BS.	Hard interference control. No D2D plus cellular links.
Mode 2: *Overlay*	Same interface as cellular. Spectrum control is in BS. No cellular interference.	Waste of cellular resources. No D2D plus cellular links.
Mode 3: *Outband*	No cellular interference. Own MAC protocol. Concurrent cellular & D2D links.	Two interfaces in UEs. Harder energy management.

transmission modes to WiFi mode and viceversa, it is important to analyze the complexity overhead of supporting multi-mode frameworks. Asadi *et al.* [11, 12] have experimentally computed the cross-platform delay suffered by a packet that is received by the LTE MAC and processed to the WiFi MAC in a real FPGA-based testbed. This time is of the order of very few milliseconds (below 3 ms), which jointly with the low delay incurred due to LTE and WiFi transmissions complies with the suggested 3GPP delay budget of 70 ms for end-to-end packet delivery [24]. As a result, it is reasonable to assume that a UE is able to switch from one mode to another.

Li *et. al.* [21] propose the use of vertex coloring to jointly perform mode selection and resource allocation in underlay D2D networks. Although they do not model the relay of traffic through underlay D2D, the insights of [21] are relevant to us in order to compare our results with the MSP where the only D2D mode enabled is *Inband Underlay*. Conversely, Zhang *et al.* [20] propose GMD2D, a D2D framework where the network performs mode selection in the presence of overlay D2D communications. In [20], D2D users establish connections either though cellular links or trough D2D overlay links. In the latter case, the dedicated spectrum may be *divided* or *shared* among D2D users, but always orthogonal to cellular channels. The insights of [20] are also relevant to us in order to compare MPD2D with frameworks where the only D2D mode enabled is *Inband Overlay*.

Wen *et al.* [25] develop a scheme for mode selection over both *Inband D2D* modes, but they focus on maximizing aggregated network throughput with no energy constraints on users, and impose QoS constraints. Maghsudi *et al.* [26] propose a distributed scheme to approach the MSP on both *Inband* modes where the users are the entities making decisions. However, authors need to over-simplify their problem to find such a distributed solution. Khan *et al.* [27] also study the same scenario, although they propose a scheme in which a circular cell is divided in inner and outer disks for cellular and D2D users, respectively. However, users cannot demand for traffic from multiple entities, only from one neighbor or from the BS. Thus, cellular and D2D users sets are disjoint. Finally, Della *et al.* [28] propose a convex optimization program to solve mode allocation in TDD (Time Division Duplex) systems with one D2D pair transmitting under licensed spectrum.

Table 2: List of acronyms

Acronym	Meaning
3GPP	3rd Generation Partnership Project
4G, 5G	Forth/Fifth Generation
AIIS	Accumulated Individual Indicator of Satisfaction
BS	Base Station
D2D	Device-to-Device
DEMA	Dynamic Exponential Moving Average
DEMM	D2D Expeditious Multimode Multi-path
DIMM	D2D Intensive Multimode Multi-path
EMA	Exponential Moving Average
eNB	evolved Node B
eProSe	Proximity-based Services
FBD2D	Floating Band D2D
GMD2D	Group D2D Mode
IIS	Individual Indicator of Satisfaction
LTE	Long Term Evolution
MCS	Modulation and Coding Scheme
MILP	Mixed Integer Linear Program
Mode 0	Cellular Mode
Mode 1	Inband Underlay Mode
Mode 2	Inband Overlay Mode
Mode 3	Outband Mode
MPD2D	Multi-Path D2D
MSP	Mode Selection Problem
OFDMA	Orthogonal Frequency Division Multiple Access
QoS	Quality of Service
SDR	Software-Defined Radio
SINR	Signal-to-Interference-plus-Noise Ratio
TDD	Time Division Duplex
UE	User Equipment

Table 3: List of variables

Variable	Description
α	Parameter for EMA
α_s	Scaling factor: cost of bit per Joule
β_{lte}	Baseline energy of LTE
β_{idle}^{WiFi}, β_{active}^{WiFi}	Baseline energy of idle/active WiFi
$B_{n,m}^{i}(j)$	Number of RBs for link (n,m) in mode i
E	Energy consumption
$\mathcal{F}$	Set of flows
$f_n(j)$, $F_n(j)$	IIS in j, AIIS in j
$I_{x,m}^{i}$	Interference from x to m in mode i
$\mathcal{L}(j)$, $\mathcal{L}^{D2D}$	Set of potential links, Set of D2D links
μ	Parameter for DEMA
$\mathcal{N}$, $\mathcal{N}^*$	Set of users, Set of nodes
$\mathcal{N}_u$	Set of D2D neighbours of $u \in \mathcal{N}$
$\mathcal{P}_f(j)$	Set of paths that flow f can follow
$p_{Tx}^{i}(x)$	Power transmission of x in mode i
$p_{u_M}^{k,M}$	Energy in one subframe in LTE modes
$p_{u_M}^{3,M}$	Energy per bit in WiFi mode
R_C, R_{D2D}	Cell radius, D2D range
$R_{n,m}^{i,CSI}(j)$	Bits sent per RB in LTE modes
$R_{n,m}^{3,CSI}(j)$	Bits per second in WiFi mode
T	Time interval
θ	Throughput
t_{idle}^{act}	Time to activate an idle WiFi card
$\mathcal{T}_m^i$	SINR threshold for m in mode i
$U_n(j)$	Utility of node n in time interval j
$U_{net}(j)$	Network utility in time interval j
$w_k(j)$	Weights for DEMA and EMA
Y	Binary variable: utilization of a link
$z(j)$	Utility function of the optimization in j

Datsika *et al.* [22] propose a cross-network architecture of *Outband* D2D cellular networks, where D2D exploits unlicensed spectrum to relay traffic from the core of the network. By building on IEEE 802.11 mechanisms for channel contention, the authors design an efficient cooperative protocol for *Outband* D2D in one cell. Traffic is efficiently delivered to end-users by means of D2D relays. Here, the use of *Outband* mode as the only D2D enabled mode is relevant to us in order to compare MPD2D to D2D schemes that only consider WiFi Direct when performing D2D communications. Asadi *et al.* deploy and study in [29] an interesting architecture based on WiFi Direct integrated to 5G networks. Although they do not consider *Inband* D2D modes, they analyze clustering of D2D users to relay cellular traffic through *Outband* mode, and implement it with an SDR (Software-Defined Radio) testbed.

Authors of [19] propose FBD2D, an innovative framework in which the BS adaptively selects which D2D mode each

UE should use for global benefit in a cell. Depending on the scenarios and users density, different D2D modes are allocated to links. For instance, co-channel interference of a microcell spoils *underlay* D2D links, while *outband* WiFi D2D performs better due to the contention of the channel with collision avoidance strategies. Also, low D2D density wastes the *overlay* portion, so that the cellular performance is uselessly decreased. Then, a scenario with heterogeneous communication technologies emerges, facing the well-known *D2D mode selection problem*. However, assumptions of FBD2D limit the capabilities of the network. First, FBD2D enforces UEs to use only one wireless interface at a time. Second, FBD2D mainly aims to activate links (cellular or D2D) that connect two nodes without constraints on flows, so that some communications will be likely disrupted. Lastly, FBD2D operates in slotted time, so that every T seconds the scheme optimizes network performance by means of activating links in the next time interval. Nevertheless, in a static scenario the allocation remains the same, so there are links much less utilized that suffer unfair treatment from the network.

All these works do not address the *D2D mode selection problem* as comprehensively as we do. In fact, we couple *Outband* mode through WiFi technology, exploit the capabilities of a network with multiple D2D modes enabled where UEs can use several interfaces at once, and account for flow demands accomplished through relaying over multiple D2D paths. Besides, we raise satisfaction of cell flows thanks to our newly designed *satisfaction metric*.

In order to ease the reading of the paper, we have listed in Table 2 the meaning of all the acronyms and in Table 3 the description of all the variables used along this paper.

3. Using D2D Links to Create Multiple Data Paths

In this section we present *Multi-Path D2D (MPD2D)* as well as the system model and the assumptions we take on D2D-enabled networks. We also model network features and maximize a network utility function based on throughput, energy consumption, and user satisfaction. Finally we present our mathematical optimization problem.

3.1. System Model

We consider a hexagonal 3GPP OFDMA D2D-enabled cell with an evolved Node B (eNB) placed in the middle as the BS. The cell is inscribed in a circumference of radius $R_C{>}0$ where a set of UEs $\mathcal{N}$ are placed (see Figure 1). The technology used for *outband* D2D is WiFi. We assume that all UEs have both interfaces, cellular and WiFi, although the scheme can be easily extended to having some UEs with only one interface, or more than two. When two UEs are closer than a D2D pre-defined range $R_{D2D}{>}0$ they can establish a D2D connection and become D2D neighbors. Given two UEs in D2D range, we assign to their link a probability of being D2D neighbors based on distance. Then, let $P{:}\,[0,\ R_{D2D}] \to [0,1]$ be a decreasing function, two UEs $u_1, u_2 \in \mathcal{N}$ in D2D range will be D2D neighbors with probability $P(\mathrm{dist}(u_1,u_2))$.[1] We define $\mathcal{N}_u$ as the set of D2D neighbors of UE $u \in \mathcal{N}$ in the cell.

In LTE, downlink and uplink operate separately with a fixed bandwidth. *Inband* D2D modes (either *underlay* or *overlay*) use the uplink bandwidth. For uplink cellular connections the eNB schedules one UE per subframe in a portion reserved for cellular and *underlay* connections. A D2D *inband* link uses all the dedicated bandwidth to either *underlay* or *overlay* mode, so that we manage co-channel interference based on Signal-to-Interference-and-Noise Ratio

[1] We assume that the closer two UEs are, the more likely is that they are willing to establish D2D connection.

(SINR). Hence, cellular UEs do not interfere with each other, but they do with *underlay* UEs. Moreover, D2D users in *overlay* mode do not interfere with cellular nor *underlay* users, but they do interfere among themselves. Additionally, *outband* links will not cause interference since they operate in a different band exploiting WiFi technology. Thus, they contend for the channel with well-known collision avoidance strategies from CSMA/CA protocol for IEEE 802.11, as also adopted in [22].

We introduce the presence of cell flows as those entities that need to be provided with a certain QoS. This is important since optimizing per-user throughputs and fairness would not automatically provide per-flow guarantees. When a UE wants to communicate with a device outside the D2D range (either inside or outside the cell) it will do it through the eNB according to the legacy system. Flows originated or terminated outside the cell are mapped onto the eNB as source or destination, respectively. However, if two D2D neighbors wish to communicate, they set a cell flow that must be served through a direct link and/or via the eNB. We define a set of flows $\mathcal{F}$ in which we can find three types of flows:

(i) A cellular flow from the eNB to a destination $d \in \mathcal{N}$.
(ii) A cellular flow from a source $s \in \mathcal{N}$ to the eNB.
(iii) A D2D flow from a source $s \in \mathcal{N}$ to a destination $d \in \mathcal{N}$ in D2D range.

In order to serve such flows, we allow a key feature expected to be performed on D2D communications: relaying. Then, a given flow $f \in \mathcal{F}$ may have several paths to follow. We only allow two-hop paths for each flow, and when a path of two hops takes place it must contain the eNB. This approach allows for easy network management at the eNB. Otherwise, in a multi-hop path involving only D2D users, the eNB will hardly be aware of performance regarding interference and signaling in these connections. For instance, WiFi Direct technology has been experimentally proven to be capable of relaying cellular traffic to users with low cellular access rate [12], supported by cellular signaling with the eNB. However, it poses some challenges for multi-hop D2D paths due to the hard signalling and synchronization management at the eNB, which in contrast to two-hop relayed paths, may incur non-negligible delay and data rate drops [11, 12]. This fact reinforces our choice to consider only two-hop paths in which the eNB is involved. As a matter of fact, if the eNB could have control of all D2D links, irrespectively of whether the traffic went through the eNB, it would be possible to account for multi-hop routing in our framework; however this would imply adding extra and hard-to-manage complexity in the final optimization: while two-hop paths let the optimization account for manageable (and linearizable) quadratic constraints, multi-hop paths imply having polynomial constraints that make the optimization even non-convex, hence not solvable with off-the-self optimizers. In addition, extra constraints accounting for the extra delay are needed, as well as avoiding loops in the paths. Therefore, since the goal of this paper is to analyze the potentials of relaying in a D2D framework with all the state-of-the-art D2D modes enabled, allowing for relayed paths of two-hops lets us study the gain and opportunities that this multi-mode D2D environment provides to D2D-aided cellular networks.

Clearly, users establishing D2D links for one-hop flows get the immediate benefit of performing direct and fast transmissions at lower power consumption. Additionally, as shown later in Fig. 4.a, enabling D2D relay features allows users in the system to experience much more throughput per consumed joule in comparison with non-D2D-enabled schemes. Hence, two-hop relay becomes beneficial at system level. Hence, those users performing D2D communications

for relay purposes may be offered bill discounts, and economic benefits in general, in order to incentivize sharing their battery and resources for the sake of system's performance. Note also that D2D could be activated within trustable communities (e.g., within the devices of a same group of family members, friends, etc.) where global D2D-enabled communications benefit the community.

We define for each possible flow $f = (s, d) \in \mathcal{F}$ the possible paths that f can follow:

(i) If $f = (eNB, d)$, $d \in \mathcal{N}$, there are two types of possible paths for f:

- A path $\{eNB, d\}$ with downlink cellular mode.
- Any path $\{eNB, r, d\}$ for all $r \in \mathcal{N}_d$.

(ii) If $f = (s, eNB)$, $s \in \mathcal{N}$, there are two types of possible paths for f:

- A path $\{s, eNB\}$ with uplink cellular mode.
- Any path $\{s, r, eNB\}$ for all $r \in \mathcal{N}_s$.

(iii) If $f = (s, d)$, $s, d \in \mathcal{N}$, there are only two paths for f:

- A path $\{s, d\}$ with D2D connection.
- A path $\{s, eNB, d\}$ with uplink and downlink cellular connection where eNB acts as a relay.

We divide the time in intervals of length T seconds. At the beginning of each time interval the eNB first performs *mode selection* and then *resource scheduling*. In the mode selection phase the eNB selects which links will be used according to technology, interference and flow constraints. The eNB selects these links based on the benefits for the overall performance. Resource scheduling is out of the scope of this paper and we assume the following: (i) cellular resources in mode 0 are allocated proportionally to the number of flows carried by the link; (ii) D2D underlay and overlay (modes 1 and 2) re-use the full uplink bandwidth dedicated to each mode, in each active link. WiFi resources are not scheduled and use instead a classical random access procedure with exponential backoff in case of collision.

3.2. Modelling

In this subsection we model all the parameters, variables and metrics in order to analyze the best mode allocation for links, so to maximize the network performance in terms of throughput, energy consumption and satisfaction of users.

Binary decision variables. We assume that at the beginning of each time interval $j \in \mathbb{N}$, the eNB knows the set of cell flows $\mathcal{F}(j)$. Then, the eNB builds a set $\mathcal{L}(j)$ of potentially active links. Denoting by P any of the paths described above, we define:

$$\mathcal{P}_f(j) = \{P \mid \text{flow } f \text{ can follow path } P\},$$
$$\mathcal{L}(j) = \bigcup_{f \in \mathcal{F}(j)} \bigcup_{P \in \mathcal{P}_f(j)} \{(n, m) \in P\},$$

so $\mathcal{P}_f(j)$ is the set of paths that $f \in \mathcal{F}(j)$ can follow. Over the set of links $\mathcal{L}(j)$ we define the decision variables for our scheme and whose values we want to find out in order to optimize the network.

For all nodes $n, m \in \mathcal{N}^*(j)$ such that $(n,m) \in \mathcal{L}(j)$, for all modes $0 \leq i \leq 3$, and for all time intervals $j \in \mathbb{N}$, we define $Y^i_{n,m}(j)$ as:

$$Y^i_{n,m}(j) = \begin{cases} 1, & \text{if } (n,m) \text{ is active in mode } i \text{ during } j; \\ 0, & \text{otherwise,} \end{cases}$$

where $\mathcal{N}^*(j) = \mathcal{N}(j) \cup \{eNB\}$ is the set of nodes of the cell containing the base station. Then, $\{Y^i_{n,m}(j)\}$ is the set of binary decision variables.

Furthermore, to evaluate the energy consumption of WiFi active links, we define an extra set of binary decision variables to tell whether the state of the WiFi interface during time interval $j \in \mathbb{N}$ is idle or the transceiver is used. For mode $i = 3$ and for all UE $n \in \mathcal{N}(j)$ we define $Y^3_n(j)$ as:

$$Y^3_n(j) = \begin{cases} 1, & \text{if } n \text{ uses the WiFi transceiver during } j; \\ 0, & \text{otherwise.} \end{cases}$$

Throughput modelling. Given a link $(n,m) \in \mathcal{L}(j)$, $\theta^i_{n,m}(j)$ denotes the amount of bits that n would transmit to m in mode $0 \leq i \leq 3$ in time slot j. We model $\theta^i_{n,m}(j)$ as:

$$\theta^i_{n,m}(j) = B^i_{n,m}(j) R^{i,CSI}_{n,m}(j), \qquad 0 \leq i \leq 2; \tag{1}$$

$$\theta^3_{n,m}(j) = T \cdot R^{3,CSI}_{n,m} Y^3_n(j-1) + (T - t^{act}_{idle}) R^{3,CSI}_{n,m}(j) \left(1 - Y^3_n(j-1)\right); \tag{2}$$

where $B^i_{n,m}(j)$ is the number of resource blocks allocated to link (n,m) and $R^{i,CSI}_{n,m}(j)$ is the number of bits sent per resource block, which depends on the Modulation and Coding Scheme (MCS) and SINR, when $0 \leq i \leq 2$. $R^{3,CSI}_{n,m}(j)$ is the WiFi rate in bps and depends on the number of stations using WiFi. Our throughput model extends what derived in [19] for FBD2D. Unlike previous models, we introduce the time t^{act}_{idle} needed to activate an idle WiFi card, which is the price to pay for the *routing context switch* of (part of) a flow, e.g., to allow for (partial) traffic transfer from cellular to WLAN interfaces in a multi-homed terminal. Hence, in case that a user activates its WiFi card in the current time slot, t^{act}_{idle} accounts for a small pause in service, so that the effective time in which we account for the throughput enjoyed by the user is $T - t^{act}_{idle}$, as shown in Eq. (2).

Energy consumption modelling. To model how much energy UEs consume per each mode $0 \leq i \leq 3$ during $j \in \mathbb{N}$, we denote as $E^{i,Tx}_{n,m}(j)$ and $E^{i,Rx}_{m,n}(j)$ the energy spent by $n \in \mathcal{N}(j)$ when she connects to $m \in \mathcal{N}^*(j)$ in mode i during interval j to respectively transmit or receive data. Let $M \in \{Tx, Rx\}$, we model $E^{i,M}_{u_{Tx},u_{Rx}}(j)$ as:

$$E^{\kappa,M}_{u_{Tx},u_{Rx}}(j) = (\beta_{lte} + \beta^{WiFi}_{idle}) \cdot \left(1 - Y^3_{u_M}(j)\right) + p^{\kappa,M}_{u_M} t_{B^{\kappa}_{u_{Tx},u_{Rx}}}(j); \tag{3}$$

$$E^{3,M}_{u_{Tx},u_{Rx}}(j) = \left(\beta_{lte} + \beta^{WiFi}_{active}\right) + p^{3,M}_{u_M} \theta^3_{n,m}(j); \tag{4}$$

where $\kappa \in \{0,1,2\}$, β_{lte}, β^{WiFi}_{idle}, and β^{WiFi}_{active} are the baseline energy consumptions in a time interval of length T by LTE, idle WiFi and active WiFi interfaces respectively. For LTE ($\kappa \in \{0,1,2\}$), $p^{\kappa,M}_{u_M}$ ($M \in \{Tx, Rx\}$) is the energy consumed in one subframe for transmission and reception of data, and $t_{B^{\kappa}_{u_{Tx},u_{Rx}}}(j)$ is the number of used subframes. For WiFi ($i = 3$), $p^{3,M}_{u_M}$ is the energy consumed for $M \in \{Tx, Rx\}$ per bit during j. Regardless whether a user had her WiFi card activated in the previous time slot, β^{WiFi}_{active} accounts for the full energy consumption in the time interval

when the user uses the WiFi interface during the full time slot, as well as when the user spends a fraction of the time interval, t^{act}_{idle}, to activate the WiFi card. Please note that in the latter case, we account for user energy consumption while the card is being activated (i.e., during the pause in service).

Interference. We build an array $I^i_{x,m}(j)$ that stores the interference that $x \in \mathcal{N}(j)$ causes to $m \in \mathcal{N}^*(j)$ when she transmits in mode i during j. We consider the well-known path-loss model for wireless transmissions [30]:

$$I^i_{x,m}(j) = p^i_{Tx}(x) \cdot 10^{\frac{-PL(\text{dist}(x,m))}{10}}, \tag{5}$$

where $p^i_{Tx}(x)$ is the power of the signal that x used to transmit in mode i, and $PL(\text{dist}(x,m))$ is the path-loss in decibels (dB) which depends on the distance between x and m during j [31].

3.3. System utility functions

First, we define a node utility function $U_n(j)$ for all users and for the base station. $U_n(j)$ plays a vital role in the definition of the *satisfaction metric* that we will define later. We make $U_n(j)$ account for throughput enjoyed and energy consumed during a slotted time interval j:

$$U_n(j) = \sum_{i=0}^{3} \sum_{m|(n,m)\in\mathcal{L}(j)} \left(\theta^i_{n,m}(j) - \alpha_s E^{i,Tx}_{n,m}(j)\right) \cdot Y^i_{n,m}(j) + \sum_{i=0}^{3} \sum_{m|(m,n)\in\mathcal{L}(j)} \left(\theta^i_{m,n}(j) - \alpha_s E^{i,Rx}_{m,n}(j)\right) \cdot Y^i_{m,n}(j), \tag{6}$$

where θ represents throughput, E energy, $\alpha_s > 0$ is a scaling factor for the cost of energy per bit, Y is a binary variable representing the utilization of a link, and the summations extend over network links. Only those links $(n,m) \in \mathcal{L}(j)$ that are active (set to 1) have relevance on the node's utility, which is expressed in bits (per interval T). With the above, the global network utility function of the system in a time slot is:

$$U_{net}(j) = \sum_{n\in\mathcal{N}^*(j)} U_n(j),$$

where $\mathcal{N}^*(j) = \mathcal{N}(j) \cup \{eNB\}$ is the set of nodes in the cell at time j jointly with the base station itself.

$U_{net}(j)$ accounts for the aggregated throughput and energy consumption of all nodes in the cell. Our aim is to decide link activations in order to maximize $U_{net}(j)$. Then, $U_{net}(j)$ will be the main part of the objective function of our optimization problem, jointly with the satisfaction metric defined next.

3.4. System satisfaction.

We introduce satisfaction indicators to measure how users exploit the network over time in order to bias link allocation decisions by following the principles of proportional fair schedulers. When using such schedulers, links acquire priority when they are in good transmission conditions and if they have been underutilised.

For every time interval $j \in \mathbb{N}$, and for every node $n \in \mathcal{N}^*(j)$, we compute an *individual indicator of satisfaction* (IIS), namely $f_n(j)$. This indicator tells how good the experience of node n was during interval j. Since the node utility function $U_n(j)$ depends on the decisions made during j and on throughput experienced and energy consumed, a natural definition for IIS is $f_n(j) := U_n(j)$.

Depending on the history of a user, we derive an *accumulated individual indicator of satisfaction* (AIIS), namely $F_n(j)$. This value $F_n(j)$ indicates how good the experience of n has been in the previous $j-1$ time intervals. Then, we filter $\{f_n(k)\}_{k=1}^{j-1}$ to obtain $F_n(j)$ with a weighted average:

$$F_n(j) = \sum_{k=1}^{j-1} w_k(j) f_n(k), \quad \text{where } \sum_{k=1}^{j-1} w_k(j) = 1.$$

Weights increase with k in an exponential-shaped form, thus concerning more about the satisfaction enjoyed in recent past. This results in a *one-step-memory* filtering process, which avoids having to store each user's full history. Let $\mu > 1$ be a real number. Using the geometric sum result we define:

$$w_k(j) := \frac{\mu - 1}{1 - \mu^{1-j}} \cdot \mu^{k-j}, \quad \forall 1 \leq k < j, \tag{7}$$

so the sum of weights $\{w_k(j)\}_{k=1}^{j-1}$ for a fixed j is 1.

Let $\xi(j) := \frac{\mu^{j-1}-1}{\mu^{j}-1}$ for all $j \geq 1$. Then, the following recurrence for $F_n(j)$ values holds and enables a one-step memory operation:

$$F_n(j+1) = \xi(j) F_n(j) + \big(1 - \xi(j)\big) f_n(j), \quad \forall j \geq 1. \tag{8}$$

We name our proposal of a one-step-memory filtering process as *Dynamic Exponential Moving Average* (DEMA), since it results to be a novel extension of the well-known exponential moving average (EMA) [32]. Unlike EMA, we have dynamic coefficients for each IIS that are adapted to the lifespan of a flow in the system. As we show below, thanks to the use of dynamic weights, DEMA reacts very quick to changes in nodes' satisfaction. For convenience, we also name as $w_k^{DEMA}(j)$ the weights and $F_n^{DEMA}(j)$ the AIIS values of the DEMA scheme.

In order to average satisfaction values over time with no bias on new arrivals and short-lived flows, we have derived DEMA with no intention to resemble EMA. Hence, to remark the differences between both schemes and the novelty of DEMA, we provide a comparison discussion between both schemes in Appendix A.

4. Optimization of Flow Allocation over D2D Links and Modes

4.1. Objective Function

We maximize the network utility $U_{net}(j)$ in a proportional fair way. Therefore, we include AIIS values $F_n(j)$ in the objective function in order to prioritize users not only according to their instantaneous utility, but also according to their satisfaction history. Then, the lower $F_n(j)$ is for a user's flow n, the higher we make its contribution to the overall performance:

$$z(j) = \sum_{n \in \mathcal{N}^*(j)} \frac{U_n(j)}{F_n(j)}.$$

Please note that the utility function is a combination of throughput and energy metrics, weighted by means of AIIS values and binary decision variables (Y). As we aim to maximize system throughput while minimizing energy consumption, we have combined the throughput achieved in the reference interval (θ) and the energy consumption (E) by means of a scaling factor (α_s), as shown in Eq. (6), which expresses the economical value of a bit of data with

respect to the cost of energy. Once formulated the optimization program, such an approach on the utility function provides Pareto-optimal solutions, i.e., the found optimal solution is such that throughput cannot be increased without increasing energy consumption and energy consumption cannot be deceased without decreasing throughput [33]. Hence, our formulation provides the optimal solution searched in such a multi-objective optimization problem. Please see Appendix C for further details.

4.2. Network Constraints

MPD2D is restricted to some conditions that result in three kinds of constraints for the optimization problem:

Technology constraints. In LTE (and 3GPP cellular networks in general) a node can set a direct link (either cellular or D2D) with only one other node of the cell. Then, a node n can only use one of the LTE modes: mode 0 (celluar), mode 1 (*underlay*) or mode 2 (*overlay*). Independently she can use also mode 3 (*outband*).

Interference constraints. In a D2D-enabled network there is co-channel interference that can spoil network performance. Then, we impose SINR thresholds in the form of optimization constraints.

Let $n \in \mathcal{N}(j)$, $m \in \mathcal{N}^*(j)$, and $0 \leq i \leq 2$, and let $\mathcal{T}_m^i > 0$. We want that the SINR experienced in link (n, m) in mode i is above $\mathcal{T}_m^i$ in order to ensure good QoS in cellular connections. We give values to these thresholds according to the implication they have in the lowest MCS guaranteed to users [34].

Flow constraints. We impose the service of flows in $\mathcal{F}(j)$, defined in Section 3.1, through relaying data over multiple D2D paths.

4.3. MPD2D Optimization Problem

The resulting MPD2D optimization problem is shown in what follows. For ease of readability we denote $e = eNB$ and omit j-dependence.

$$
\begin{cases}
\max \quad z = \displaystyle\sum_{n \in \mathcal{N}^*} \frac{U_n}{F_n}; \\
\sum_{i=0}^{2} \sum_{m|(n,m)\in\mathcal{L}} Y_{n,m}^i \leq 1, \ \forall n \in \mathcal{N}; \\
\sum_{m|(n,m)\in\mathcal{L}} Y_{n,m}^3 \leq 1, \ \forall n \in \mathcal{N}; \\
\sum_{i=0}^{2} \sum_{n|(n,m)\in\mathcal{L}} Y_{n,m}^i \leq 1, \ \forall m \in \mathcal{N}; \\
\sum_{n|(n,m)\in\mathcal{L}} Y_{n,m}^3 \leq 1, \ \forall m \in \mathcal{N}; \\
\sum_{(t,r)\in\mathcal{L}} Y_{n,e}^0 Y_{t,r}^1 I_{t,e}^1 \leq \gamma_{n,e}^0, \ \forall n \in \mathcal{N} \mid (n,e) \in \mathcal{L}; \\
\sum_{i=0}^{1} \sum_{(x,y)\in\mathcal{L}\setminus\{(n,m)\}} Y_{n,m}^1 Y_{x,y}^i I_{x,m}^i \leq \gamma_{n,m}^1, \ \forall (n,m) \in \mathcal{L}; \\
\sum_{(x,y)\in\mathcal{L}\setminus\{(n,m)\}} Y_{n,m}^2 Y_{x,y}^2 I_{x,m}^2 \leq \gamma_{n,m}^2, \ \forall (n,m) \in \mathcal{L}; \\
Y_n^3 = \min\left(1, \sum_{m \mid (n,m)\in\mathcal{L}} Y_{n,m}^3 + \sum_{m \mid (m,n)\in\mathcal{L}} Y_{m,n}^3\right), \ \forall n \in \mathcal{N}; \\
\sum_{i=1}^{3} Y_{s,d}^i + Y_{s,e}^0 Y_{e,d}^0 \geq 1, \ \forall (s,d) \in \mathcal{F} \mid s,d \in \mathcal{N}; \\
Y_{e,d}^0 + \sum_{r \mid (r,d)\in\mathcal{L}} \left(Y_{e,r}^0 \sum_{i=1}^{3} Y_{r,d}^i\right) \geq 1, \ \forall d \in \mathcal{N} \mid (e,d) \in \mathcal{F}; \\
Y_{s,e}^0 + \sum_{r \mid (s,r)\in\mathcal{L}} \left(Y_{r,e}^0 \sum_{i=1}^{3} Y_{s,r}^i\right) \geq 1, \ \forall s \in \mathcal{N} \mid (s,e) \in \mathcal{F}.
\end{cases}
\tag{9}
$$

The first four constraints model technology constraints. The first two are for transmitters and the next two for receivers. It follows the set of three interference constraints. First, we manage interference from cellular users in uplink

with *underlay* D2D users in the eNB. Second, we manage interference between cellular and *underlay* D2D users in each of the D2D users. Third, we manage interference for *overlay* D2D users. The last three constraints force the optimization to serve all flows over at least one path.

The optimization problem is binary and non-linear in the objective function and in the constraints. All non-linearities can be linearized with additional binary variables and linear constraints that increase the complexity of the formulation. Hence, as shown in Appendix B, we turn the non-linear optimization program onto a Mixed-Integer Linear Program (MILP). Therefore, we can apply standard approaches as a combination of interior-point methods [35] with a *Branch&Bound* search [36] in order to solve it.

In order to reduce complexity, we propose two effective heuristics in order to approximate the optimum provided by MPD2D.

5. Heuristics: DIMM and DEMM

Algorithm 1 DIMM: D2D Instensive Multimode Multi-path

Input: $\mathcal{N}$, $\mathcal{L}$, $\mathcal{F}$: Sets of users, links and flows.
$\{I^i_{n,m}\}, \{\gamma^i_{n,m}\}$: interference parameters.
Output: $\mathbf{Y} = \{Y^i_{n,m}\}$: Set of decision variables.
Initialize:
$Y^0_{s,e} = Y^0_{e,d} = 1 \ \forall \ (s,e),(e,d) \in \mathcal{F}$
for $(s,d) \in \mathcal{F} \mid s,d \in \mathcal{N}$ **do**
  $Y^0_{s,e} = Y^0_{e,d} = 1$
  if $Y^3_{s,u} = Y^3_{u,d} = 0 \ \forall \ u \in \mathcal{N}$ **then**
    $Y^3_{s,d} = 1$
$\mathbf{Y^?} = \mathbf{Y}$; $max = z = U_{net}(\mathbf{Y})$.
while $\mathbf{Y_{old}} \neq \mathbf{Y}$ **do**
  $\mathbf{Y_{old}} = \mathbf{Y}$
  for $(n,m) \in \mathcal{L}^{D2D}$ **do**
    for $i \in \{1,2\}$ **do**
      $Y^{i,?}_{n,m} = 1; \ Y^{k,?}_{n,m} = 0 \ \forall \ k \in \{1,2\} - \{i\}$
      $Y^{k,?}_{n,u} = Y^{k,?}_{u,m} = 0 \ \forall \ u \neq n,m; \forall \ 0 \leq k \leq 2$
      $z = U_{net}(\mathbf{Y^?})$
      if $z > max$ & SINR and Flows satisfied **then**
        $\mathbf{Y} = \mathbf{Y^?}$; $max = z$
      else
        $\mathbf{Y^?} = \mathbf{Y}$
      for i=3 **do**
        $Y^{3,?}_{n,m} = 1; Y^{3,?}_{n,u} = Y^{3,?}_{u,m} = 0 \ \forall \ u \neq n,m$
        $z = U_{net}(\mathbf{Y^?})$
        if $z > max$ & Flows satisfied **then**
          $\mathbf{Y} = \mathbf{Y^?}$; $max = z$
        else
          $\mathbf{Y^?} = \mathbf{Y}$

Solving the MPD2D optimization problem shown in Eq. (9) is computationally hard. Hence we propose *DIMM* and *DEMM*, two heuristics that perform a sequential search of multiple D2D paths through multi-mode selection. As described in Algorithm 1, *D2D Intensive Multimode Multi-path (DIMM)* executes a full search of multi-paths checking SINR violation at each decision. Instead, as described in Algorithm 2, *D2D Expeditious Multimode Multi-path (DEMM)*

makes preliminary decisions based on link allocations that potentially violate SINR thresholds, so SINR constraints are assumed to be respected and no longer checked in the algorithm. Thus, *DIMM* performs more accurate mode selection while *DEMM* has lower complexity, which is desirable for scalable decision making.

Algorithm 2 DEMM: D2D Expeditious Multimode Multi-path

Input: $\mathcal{N}$, $\mathcal{L}$, $\mathcal{F}$: Sets of users, links and flows.
$\{I^i_{n,m}\}, \{\gamma^i_{n,m}\}$: interference parameters. $\rho \in]0,1[$.
Output: $\mathbf{Y} = \{Y^i_{n,m}\}$: Set of decision variables.
for $(n,t) \in \mathcal{N} \times \mathcal{N} \mid I^1_{t,e} > \rho \cdot \gamma^0_{n,e}$ **do** $\theta^1_{t,r} = 0, \forall\ r \in \mathcal{N}$
for $(n,m) \in \mathcal{L}^{D2D}$ **do**
  for $x \in \mathcal{N} - \{n\} \mid I^0_{x,m} > \rho \cdot \gamma^1_{n,m}$ **do**
    $\theta^1_{n,m} = 0$
  if $\theta^1_{n,m} > 0$ **then**
    for $x \in \mathcal{N} - \{n\} \mid I^1_{x,m} > \rho \cdot \gamma^1_{n,m}$ **do**
      $\theta^1_{x,r} = 0, \forall\ r \in \mathcal{N}$
for $(n,m) \in \mathcal{L}^{D2D}$ **do**
  for $x \in \mathcal{N} - \{n\} \mid I^2_{x,m} > \rho \cdot \gamma^2_{n,m}$ **do**
    $\theta^2_{x,r} = 0, \forall\ r \in \mathcal{N}$
Do DIMM withouth SINR checking.

Both heuristics first allocate all cellular connections to UEs to serve all flows and then add as many WiFi links among D2D users as possible in order to give flexibility when trying to move and split flows during the algorithm. Then they iterate over the set of D2D links $\mathcal{L}^{D2D}$, i.e., links that do not involve the eNB, and try to allocate sequentially each of the D2D modes to each of those links, provided that all flows are served. Besides, *DIMM* checks the SINR thresholds in order to provide feasible solutions. Conversely, *DEMM* a-priori bans any possible allocation that likely spoils any SINR constraint. To this end, we randomly sort potential links for fairness in terms of energy cost distribution across potential relays, which is also convenient since it incurs low complexity overhead. When a link allocation increases utility, *DIMM* and *DEMM* activate the link and deactivate other incompatible links, according to MPD2D constraints.

Hence, the main differences between DIMM and DEMM are the following. While DIMM directly iterates to find the best combination of allocation modes to links that maximize the utility, DEMM performs a previous banning of a set of links that potentially incur too much interference to the system, so that enabling them would not be potentially beneficial for the final performance. Such a banning is performed by means of checking a-priori whether the incurred link interference is higher than a portion of the maximum allowed interference (modelled with the parameter γ). Hence, while DIMM checks at each decision point if the whole set of interference constraints are violated or not, DEMM takes advantage of the a-priori banning and is able to assume that such constraints do not need to be checked at each decision making. Of course, this is an approximation used to considerably save complexity by using DEMM, as detailed in the complexity analysis.

Complexity Analysis. We iterate over all D2D links in $\mathcal{L}$ and calculate up to one utility per D2D mode and per link: $3|\mathcal{L}^{D2D}|$ utilities. The cost of each utility computation is linear with the number of users $|\mathcal{N}|$, since technology constraints do not allow the system to have more that $5|\mathcal{N}|$ active links in the cell.[2] Besides, *DIMM* has to check SINR

[2]Each node can have one downlink connection from the eNB, two WiFi links to transmit and receive packets to relay using the random access technique of IEEE 802.11, and one or two links using the uplink licensed band: either a connection to the eNB or a pair of

constraints, whose amount is linear with $|\mathcal{L}|$. Therefore, complexity of *DIMM* is $\mathcal{O}(5 \cdot 3|\mathcal{L}^{D2D}||\mathcal{L}||\mathcal{N}|)$, while *DEMM* has complexity $\mathcal{O}(5 \cdot 3|\mathcal{L}^{D2D}||\mathcal{N}|)$. Since $\mathcal{L}^{D2D} \subset \mathcal{L}$ and the sizes of the two sets are at most quadratic with the number of users, the complexity of *DIMM* goes with the fifth power of $|\mathcal{N}|$ while *DEMM* has a cubic dependence on $|\mathcal{N}|$.

6. Numerical Evaluation

In this section we present results for solving MPD2D and for its heuristics through numerical simulations. We study the gain of MPD2D and heuristics in comparison to the benchmarks based on D2D schemes that consider only one D2D connection mode, as GMD2D [20] (only *Inband Overlay* is enabled), Underlay MSP [21] (only *Inband Underlay* is enabled) and Outband D2D [22] (only *Outband* is enabled). Also, we compare to the cellular legacy system. Additionally, we compare FBD2D [19] (all D2D modes are enabled). We mainly study performance of throughput, energy consumption, fairness and evolution of satisfaction over time. Error bars in the graphs represent 95% confidence intervals. We allocate cellular resources to LTE links proportionally to the number of flows they carry. The amount of D2D users is not limited. Unless otherwise specified, every user has a flow coming from the eNB, and half of them have a flow towards the eNB. We place users uniformly in a hexagonal cell inscribed within a radius $R_C = 175$ m. Any pair of devices become a D2D pair with a probability that decreases linearly with their distance and becomes 0 at distances larger than R_{D2D}. Such a D2D range has to be short since it represents a reasonable distance in order to achieve high transmission gains as well as perform communications at high rates (as expected and demanded for D2D to be viable), in any of the modes. Note that long D2D ranges would require unsustainably high transmission power and incur high interference, which would impact the system performance by consuming more energy and adding extra computational cost due to harder interference management. For simplicity, in our numerical experiments, we set $R_{D2D} = 20$ m for all D2D modes, which is in line with what commonly considered in the literature [19, 21, 37, 38]. All D2D pairs may have a flow from one to the other. Any flow can follow multiple paths, as detailed in Section 3.1.

We consider as benchmark schemes for MPD2D the following cases: `Overlay`, `Underlay` and `WiFi`. In `Overlay`, the only D2D mode enabled is *Inband Overlay*, as done in GMD2D [20]; in `Underlay`, the only D2D mode enabled is *Inband Underlay*, as done in Underlay MSP [21]; and in `WiFi`, the only D2D mode enabled is *Outband*, as done in [22], by means of WiFi technology. We also compare to `Cellular`, a scheme that corresponds to sending all traffic through cellular connections, as in the cellular legacy system (D2D is not enabled). In `WiFi` scheme, the devices may also use cellular and WLAN interfaces at the same time. We adapt *DIMM* and *DEMM* to work with these three benchmarks, e.g., by disabling the selection of non-allowed D2D modes in each case.

Table 4 gathers the main parameters of the system model. We dedicate 30% of cellular resources to *overlay* mode, but leave this portion to cellular and *underlay* modes when *overlay* mode is unused. Carrier frequency for LTE is the 800 MHz band, since it is one of the bands used to deploy 4G+ in European countries (band 20) [39]. Bandwidth for downlink and uplink is of 20 MHz each. The minimum threshold for SINR is 15 dB, so that nodes may use at least a MCS with 16QAM modulation and coding rate of 3/4 [34]. The value of α_s is an estimation of the relative cost of bit with respect to the cost of a Joule in the market, as considered in the literature [19], although other values may be applied. We consider traffic queues under infinite offered load conditions in which users have always data ready to transmit, so we

incoming/outgoing D2D inband links.

Table 4: Evaluation Parameters

Parameter	***Value***
–Cell Deployment–	
Cell and D2D Range R_C, R_{D2D}	175 m, 20 m
Carrier Frequency	Band 20: 800 MHz
Cellular BW (UL & DL)	20 MHz
Overlay Portion	0.3
Time interval length T	2 secs
Time Activation WiFi Card t_{idle}^{act}	300 μs
Thermal Noise Power	-174 dBm/Hz
WiFi Rate	60 Mbps
SINR Threshold	15 dB
–Power & Energy Consumption–	
eNB/Cellular Tx Power	44 dBm / 24 dBm
D2D Inband Tx Power	10 dBm
LTE baseline β_{lte}	1288.04 mW
WiFi baseline β_{idle}^{WiFi}, β_{active}^{WiFi}	77.2 mW, 132.86 mW
WiFi power Tx/Rx	460 mW / 440 mW
Relative Cost of Energy α_s	1 bit/Joule

study the achievable performance of the system. We have used `MATLAB R2018a` to implement the MPD2D framework and heuristics so to derive the results. Concretely, in order to find optimal settings, we have used CVX [40, 41], a toolbox designed for solving optimization programs that integrates, for instance, interior-point and Branch&Bound methods. We have simulated channel conditions according to the path-loss model used in Eq. (5). User positions have been simulated according to uniform distribution within a hexagonal cell inscribed in a circumference of radius R_C=175 m. D2D associations have been set according to the analyzed scenario (D2D pairs need to be always within D2D range, but pairing depends on the scenario. For instance, we mainly test when pairing depends on a probability function than decreases linearly with the distance, as detailed later. Also, we test that users in range are always paired, et cetera). Moreover, when we test the performance of the framework over time, we simulate that users move at a speed of 4 km/h according to the well-known random way-point model, updated every T=2 s, in order to re-optimize the network. We have simulated each scenario 1000 times in order to gather average results in a personal computer.

Optimality, Throughput and Energy Consumption. In Figure 2 we show a time interval snapshot of the performance of the network utility, cell throughput and users' energy consumption. We show optimum values from 15 to 40 users. Both heuristics *DIMM* and *DEMM* provide close approximations for MPD2D and for benchmarks, while allowing to evaluate performance under a larger range of users (up to 150 in the figures reported in this paper). As expected, *DIMM* performs closer to optimum values, but it has higher complexity. Then we focus on *DEMM* for heuristic results, since it offers good approximations at quite lower cost. MPD2D clearly outperforms any other case with one single D2D connectivity path enabled. The gain of the network utility compared with `Cellular` with $|\mathcal{N}| = 40$ users is of 218%, while for the densest scenario ($|\mathcal{N}| = 150$) with *DEMM* rises up to 701%. Furthermore, *DEMM* gives a gain of 37% in comparison to `Overlay`, which offers the best results among the benchmark schemes. In conclusion, as long as we add users, DEMM results approximating the optimal MPD2D solution and enjoys much more gain than any other benchmark.

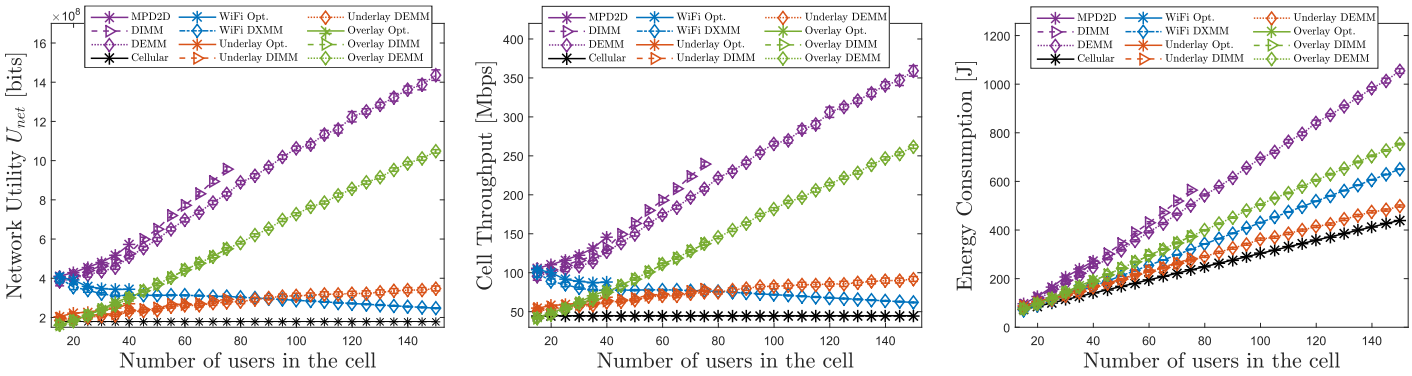

(a) Network Utility U_{net}. (b) Aggregated cell throughput. (c) Aggregated energy consumption.

Figure 2: Impact of users density on system optimality, throughput and energy consumption.

In Figures 2b and 2c we can see the specific gain of throughput and energy consumption. The shape of the throughput graph is similar to network utility since throughput is the main part of the utility function in the scheme. Throughput gain grows from 3.6% with $|\mathcal{N}| = 15$ up to 66% with $|\mathcal{N}| = 40$ in comparison with the closest benchmark, `WiFi`. With $|\mathcal{N}| = 150$, *DEMM* provides a gain of 36% in respect to `Overlay`, which for dense cells gives better throughput due to resources reuse, while WiFi usage decreases due to contention for the channel. In comparison with `Cellular`, throughput gain rises from 135% up to 702%. Besides, regarding energy consumption *DEMM* achieves up to a considerable 203% of extra cost to `Cellular`. *DEMM* is the scheme with higher energy cost due to having two interfaces enabled, since the main usage of energy is due to baseline consumption, although it saves energy compared to the exact solution of MPD2D. Nevertheless, the great gain of throughput is much higher than the extra energy cost incurred. As we observe in Figure 3a, although energy consumption is significatively increased, the time required for transmitting a full piece of data is much lower, resulting in a higher energy efficiency. Figure 3a shows how much traffic the network can transport in a second (Mbps) at the cost of one energy unit (Joule). In general, *DEMM* is the most efficient scheme compared to any benchmark. *DEMM* achieves a throughput-per-energy efficiency gain from 32% compared to `Overlay` to 82% compared to `Cellular`. Hence, the way of achieving the highest throughput and the most network efficiency is by means of the MPD2D framework.

Figure 3b sheds light on the impact of the *overlay* portion for $|\mathcal{N}| = 30$ users. We split throughput onto each connection mode in order to understand why this is the behavior. Clearly, widening the *overlay* bandwidth results into higher data rates. This shows that reuse of resources in a band with low interference helps to increase very substantially the total throughput. Moreover, with narrow *overlay* portions MPD2D and *DEMM* try to allocate D2D links over the *underlay* mode when interference is not high. However, once the *underlay* spectrum is lower than 50%, the *overlay* mode is much more preferred because it has higher bandwidth and much less interference problems, so that the *underlay* mode is barely used. WiFi throughput is not affected since this technology does not use licensed band. As evident from the figure, the *overlay* portion should be maximum to achieve the highest data rates. However, widening the *overlay* bandwidth implies reducing the band for cellular connections in uplink. MPD2D reflects this fact in the decrease of cellular throughput. Here, the cellular throughput accounts for downlink and uplink, so when the *overlay* portion is 90%, the cellular mode usage is mainly due to downlink connections. Since the QoS for uplink connections cannot

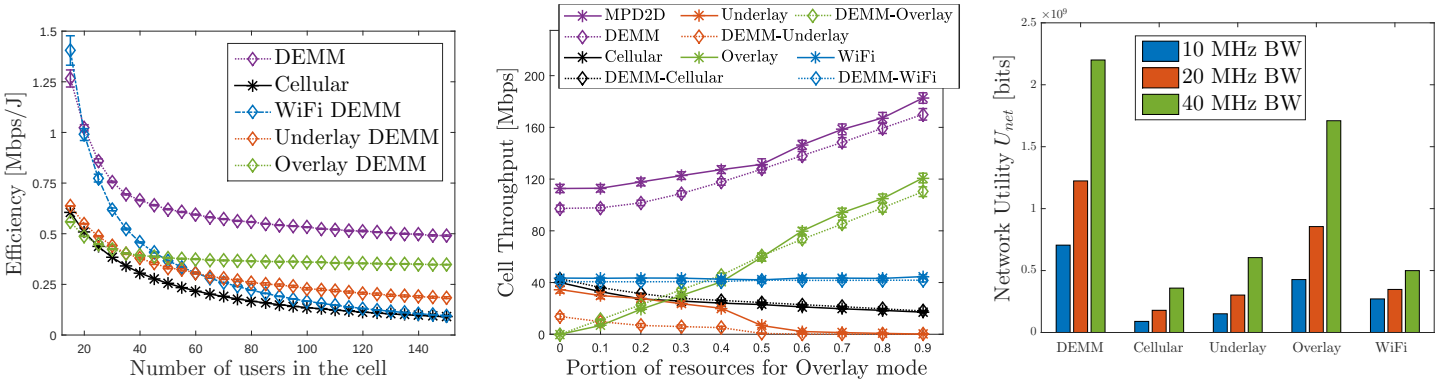

(a) Impact of users density on the ratio between throughput and energy.

(b) Impact of *overlay* portion with $|\mathcal{N}| = 30$.

(c) Impact of LTE channel bandwidth with $|\mathcal{N}| = 120$ on all D2D schemes

Figure 3: Network efficiency, impact of overlay portion and impact of LTE channel bandwidth

be much reduced, a reasonable portion for the *overlay* mode is between 30% and 40%.

In Figure 3c we show the impact of changing the LTE channel bandwidth on the network performance when we apply all different D2D schemes (with $|\mathcal{N}| = 120$ users). On the one hand, we observe that `Cellular`, `Underlay` and `Overlay` schemes get to scale the utility accordingly with the bandwidth factor. This is because, as mentioned earlier, throughput takes the major part of the utility function. Since the LTE channel is the only channel used in these schemes, Figure 3c reflects the proportional scaling with the bandwidth. On the other hand, `DEMM` and `WiFi` schemes reflect that having more LTE bandwidth slightly affects the WiFi channel performance. Since `DEMM` and `WiFi` are the only schemes using the orthogonal WiFi channel, they show that widening the LTE channel bandwidth helps on cellular mode and the *Inband* D2D modes. However, utility increases less in these cases because, specially with the `WiFi` scheme, the major part of traffic goes over WiFi D2D links, which are not affected by the LTE bandwidth widening.

We also mention that we have studied also the impact of using different LTE bands, namely the 1800 MHz band (band 3) and 2600 MHz band (band 7). However, while taking higher frequencies increases the signal attenuation, it also diminishes interference issues. In practice, all the analyzed schemes provide almost the same performance (within 1% difference) on each of the LTE bands. Hence, we conclude that MPD2D framework works regardless the cellular band used.

In Figure 4a, we analyze the throughput per flow performance in five different setups of the D2D network. Here, we consider five scenarios in which the probability of the establishment of D2D flows (i.e., flows that begin *and* end in a user) follows different policies. These five scenarios are, as labelled in Figure 4a,

- `All D2D flows`: Every pair of users that is within the D2D range, R_{D2D}, sets a D2D flow with probability 1.
- `Distance-based D2D flows`: Every pair of users in D2D range sets a D2D flow according to a probability that decreases linearly with the distance, as studied in the rest of the article.
- `D2D flow probability = 30%`: Every pair of users in D2D range sets a D2D flow with a probability of 0.3.
- `No D2D flows`: No D2D flow is set, although flows may use D2D relay.
- `D2D disabled`: No D2D flows and no D2D relay.

The first four scenarios correspond to D2D-enabled networks, while the last scenario corresponds to a legacy cellular

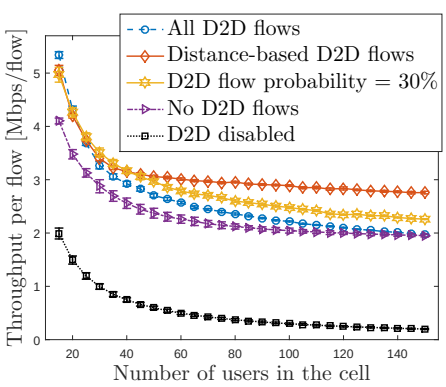

(a) Throughput per flow with different D2D flow probability distributions.

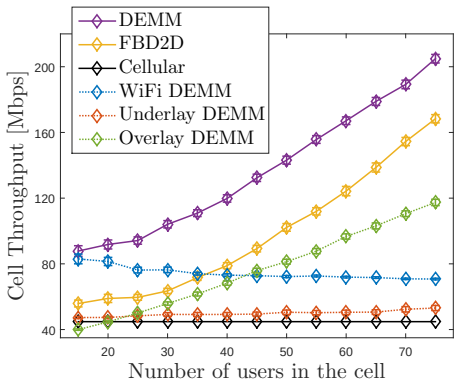

(b) Comparison of FBD2D and *DEMM*: aggregated cell throughput.

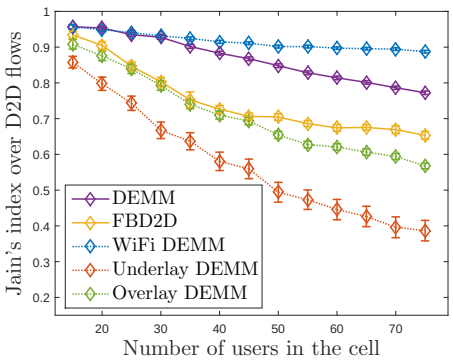

(c) Comparison of FBD2D and *DEMM*: Jain's index for the satisfaction metric, computed on D2D flows.

Figure 4: Comparison of D2D flow distributions and comparison of DEMM Vs FBD2D.

system without D2D relay. In Figure 4a, first of all we observe that per-flow throughputs decay relatively fast as the number of users that share the same resources increases. However, we observe a large gap between D2D-enabled and legacy scenarios. This happens because the D2D modes considered allow to reuse transmission resources and to add extra resources (e.g., WiFi). Indeed, using D2D brings a large gain even in absence of D2D flows. Moreover, D2D flows can further exploit spectral reuse and outband communications to establish fast links without harming cellular flows and relay operations, as it is clear from the figure. This means that D2D channels offer extremely valuable and flexible resources in all cases. Figure 4a shows that the per-flow throughput achieved in the D2D-enabled scenarios is at least double and up to ten-fifteen times higher than the one of the legacy scenario. The case of `Distance-based D2D flows` behaves better than the other D2D cases reported here. Therefore, the result tells that extreme cases with all or no D2D flows, or a case in which D2D flows are blindly established without accounting for the distance, are far from being optimal in terms of throughput. Furthermore, we can observe that in non-extreme scenarios, as `Distance-based D2D flows` and `D2D flow probability = 30%`, MPD2D is able to wisely manage the resources and D2D opportunities due to lower interference levels than the `All D2D flows` scenario, and higher traffic demand than the `No D2D flows` scenario.

The analysis conducted in the manuscript focuses on single-cell scenarios, as formulated in the optimization (9). Nevertheless, the MPD2D framework can be extended to apply to multiple cells coordinated under the same network using a network controller. Such an extension comes at the cost of extra complexity, due to user population increase, the presence of cross-border D2D links, and the augmented number of links to consider for inter-cell interference management in general. Yet the complexity would be manageable for few cells. However, DIMM will suffer severe scalability problems, whereas most of the potential interfering links added because of considering multiple cells, e.g., the ones due to users located in different and distant cells, would be efficiently labeled as non-relevant by DEMM. Using DEMM in a multi-cellular scenario would therefore result in applying DEMM to each cell, in which a few extra links from interfering neighboring cells are accounted for. Deploying a distributed DEMM would therefore be possible and efficient. In general, light complexity approaches as DEMM would offer viable solutions for large scale deployments.

Comparison with Floating Band D2D. Now we compare MPD2D with FBD2D [19]. FBD2D restricts each user to activate only one link for transmission and only one link for reception of data. Then, imposing that all flows

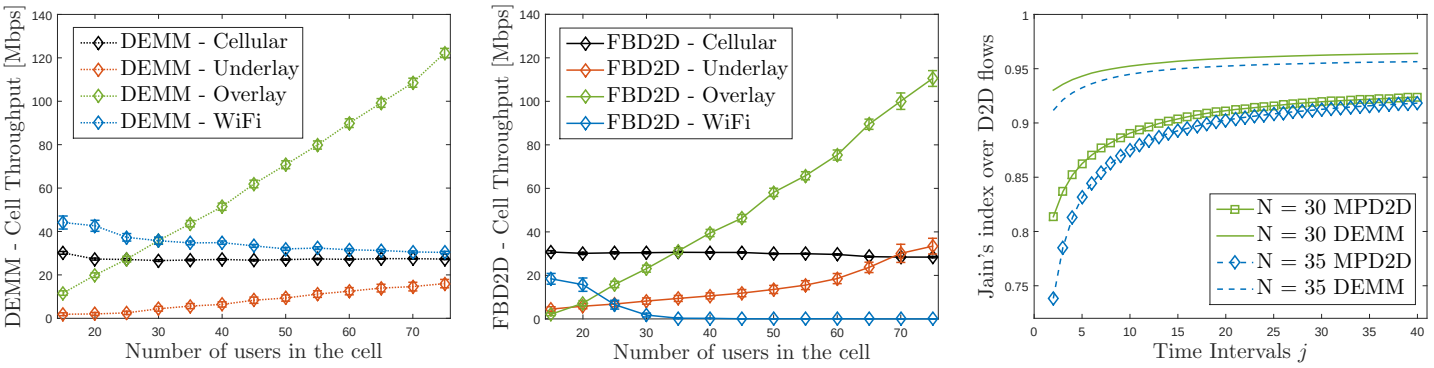

(a) *DEMM* throughput splitting (b) FBD2D throughput splitting (c) Jain's index of static D2D users.

Figure 5: Impact of users density on DEMM and FBD2D throughput splitting, and impact of time on fairness of a dynamic cell.

from eNB were served would make very likely that most of the users activated a cellular link and missed lots of D2D chances. Therefore, we deploy a different scenario in which users set half of all the possible cellular flows in uplink and also in downlink. This deployment makes it possible to compare MPD2D and FBD2D when the latter can be used.

In Figures 4b and 4c we study the impact of network density jointly with mentioned benchmarks. Both *DEMM* and FBD2D increase throughput because they raise D2D opportunities. Clearly, *DEMM* largely outperforms FBD2D, due to the main difference between both schemes: the permission to use two interfaces for D2D. Indeed, since `WiFi` also allows two interfaces at once, FBD2D performs worse than `WiFi` until we get to a dense network and WiFi performance decays, but FBD2D still outperforms the cellular and *Inband* D2D schemes. This proves the importance in MPD2D for allowing both active interfaces (LTE and WiFi) so as to drive flows over multiple paths. Schemes like FBD2D and schemes with only one D2D mode enabled hardly split flows over multiple paths due to limited use of interfaces. For instance, `Overlay` scheme does not allow a user to send data to the eNB and also transmit through *Overlay* D2D mode because both links use the same interface (LTE). Neither FBD2D allows. In fact, FBD2D explicitly states that only one interface can be used to transfer data. Conversely, MPD2D exploits the opportunity of enabling LTE and WiFi interfaces at once. Hence, MPD2D speeds up communications by means of splitting flows over multiple paths.

In order to study the network satisfaction, we compute the Jain's index [42] over satisfaction values. Let $\mathcal{M} \subseteq \mathcal{N}^*$ be a subset of the nodes, the satisfaction rate over this set is:

$$J_{\mathcal{M}} = \frac{\left(\sum_{m \in \mathcal{M}} F_m(j)\right)^2}{|\mathcal{M}| \cdot \sum_{m \in \mathcal{M}} F_m(j)^2}, \tag{10}$$

where $F_m(j)$ are the AIIS values from Section 3.4. As depicted in Figure 4c, *DEMM* performs quite better than FBD2D, since with DEMM the satisfaction remains between 0.77 and 0.96, while with FBD2D it decays from 0.96 to 0.65 as the network density increases. For cellular users we do not show the results because they are very similar. The integration of our *satisfaction metric* increases satisfaction over time to all users to much higher indices, as shown later.

Figures 5a and 5b compare the throughput allocation from FBD2D and *DEMM* into all the connection modes. They reflect the advantages and drawbacks of each mode shown in Table 1 and why the system model of MPD2D is more flexible to achieve higher data rates. Figure 5a shows that *Inband* usage rises up until SINR limits *underlay* links. Instead, interference affects much less the *overlay* mode, and WiFi mode contributes significantly to overall throughput.

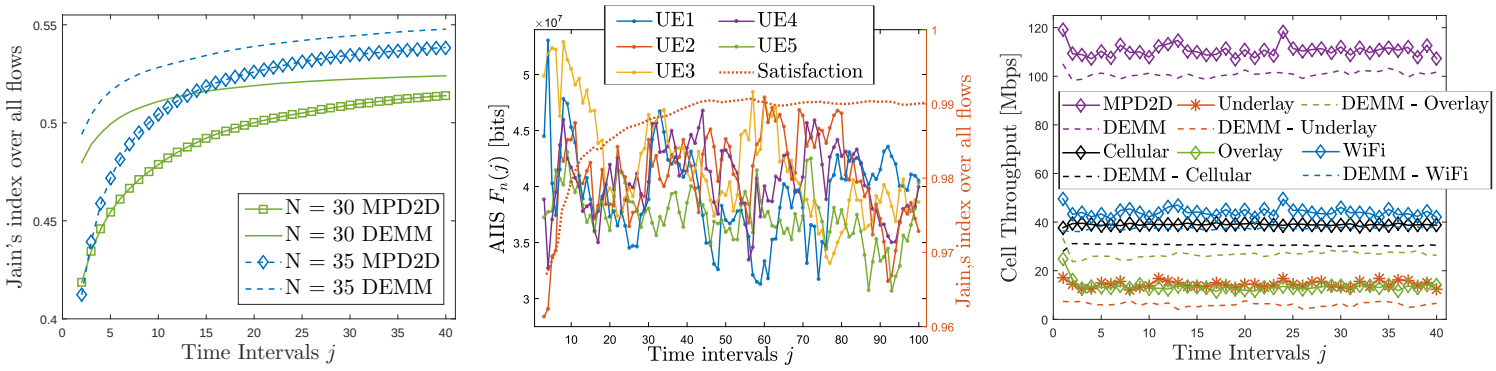

(a) Jain's index of dynamic users.

(b) Individual satisfaction evolution, $|\mathcal{N}| = 5$ users.

(c) Throughput in a dynamic cell, $|\mathcal{N}| = 30$.

Figure 6: Fairness over time, network satisfaction and throughput performance over time.

In addition, Figure 5b shows that in FBD2D WiFi degrades very quickly in benefit of *Inband* modes, since FBD2D can choose only one technology. In particular, *overlay* links are more convenient due to easier SINR management. We conclude that our scheme does not need to discard any D2D mode since MPD2D can couple and use them at the same time, which results in a much higher achievable throughput.

Fairness and Satisfaction. Figures 5c and 6a depict the effects of integrating the satisfaction metric developed in Section 3.4 onto the decisions over time in the cell. In Figure 5c we plot the Jain's index for D2D flows satisfaction in a static scenario, in which the set of D2D users does not change over time. Conversely, in Figure 6a we plot the Jain's index over all flows in a mobile scenario. Note that mobile users can be D2D or cellular users in different time intervals. For simplicity, we assume a fixed walking speed of 4 km/h for users moving during $T = 2$ s in random directions, for 40 consecutive time intervals.

Figures 5c and 6a show an great behavior of satisfaction over time with MPD2D and *DEMM*. Static D2D users increase by 18% their indices when $|\mathcal{N}| = 35$, from 0.74 up to 0.92, while the dynamic users altogether raises the satisfaction indices from 0.41 up to 0.54. In this case the Jain's index cannot be as high as in the static case, since connection opportunities are different for D2D and cellular users over time. The lesson learnt from this experiment is twofold: (i) multi-path is key to boost fair satisfaction of static D2D nodes to the limit, whilst (ii) mobile nodes experience a dramatic increase of satisfaction. Interestingly, our heuristic *DEMM* is fairer than the optimal solution of MPD2D, which is due to the fact that, as shown in Figure 6c, *DEMM* uses more WiFi and less underlay links, the latter being the well-known cause of unfair behaviors among flows.

In Figure 6b we focus on a simpler example in order to make more visual the effects that the satisfaction metric has on average on the network, as seen in Figures 5c and 6a. Here, we consider a cell with five users forming a circle inside the D2D range, so that we can establish D2D flows. Since the network is small and not complex, we apply the optimum MPD2D scheme. We locate the users in a circle in order to balance D2D connection opportunities across users. Such locations are at a distance of $R_C - 2R_{D2D}$ meters from the eNB. We take such location in order to decrease the quality of signal from cellular connections. Otherwise, when users are too close to the eNB, cellular links are selected with higher probability in this simple example and the effect of the satisfaction metric is less visible. In Figure 6b we observe the individual behavior of the satisfaction of each of the five users, as well as the performance of the Jain's index for the satisfaction of the network. The initial stage used in the experiment is a configuration under which the network utility is optimized for flows started exactly one slot before. Afterwards, the satisfaction metric gathers the experience of the

flows and, following the principles of proportional fair allocation of resources, it enforces the network to increase the satisfaction while the global performance does not decay, as depicted in Figure 6c. We see that, despite some users have better channel conditions and better paths for the flow demands, the satisfaction metric leads the system to make fairer decisions so that the individual satisfaction of the well-satisfied flows decays to leave space and increase satisfaction for other flows. As a result, the global system satisfaction increases over time, achieving nearly complete fairness.

Finally, in Figure 6c we analyze the cell throughput enjoyed over time in a dynamic network. We show also how throughput is split into connection modes to see how the satisfaction metric affects to allocation over time. This graph is very important to see that, despite the objective function does not account for actual throughput and energy consumption, throughput does not decrease to low values as time passes by. Instead, we observe very positive results in which throughput remains stable in a reasonable variation of 15 Mbps during 80 seconds. In order to increase satisfaction, the number of *overlay* D2D links is quickly decreased in benefit of cellular connections. Still, each connection mode remains quite stable over time as the aggregated throughput does.

7. Conclusions

We have proposed Multi-Path D2D (MPD2D), a D2D framework in which D2D modes are accounted for adaptive mode selection with flows split over multiple D2D paths. Results obtained show an extremely high gain in terms of throughput in comparison to state of the art schemes facing the D2D mode selection problem. The use of multiple paths is the first key contribution of this work. Although it comes with several technology restrictions, yet it shows significant potential gain that it is worth exploring. As a second key contribution, we have derived a system analysis framework and in particular we have introduced a flow satisfaction metric that provides memory to the system to make fairer link allocation decisions according to the proportional fairness paradigm, with no bias for freshly arrived flows and for short-lived flows. By defining a new filtering technique, namely DEMA, we have reduced to the minimum the implementation costs of fast reactive memory-enabled mode selection decisions in dynamic contexts. To further reduce complexity, we have proposed *DIMM* and *DEMM*, two effective heuristics that achieve close-to-optimum results and carry out mode selection in a way that largely outperforms state of the art solutions.

Acknowledgment

The work of E. Arribas is partially supported by the FPU15/02051 grant from the Spanish Ministry of Education, Culture and Sports (MECD). The work of V. Mancuso is supported by the Ramón y Cajal grant (ref: RYC-2014-16285) from the Spanish Ministry of Economy and Competitiveness and by the DiscoEdge grant (TIN2017-88749-R) from the Spanish Ministry of Science, Innovation and Universities.

References

[1] E. Arribas, V. Mancuso, Multi-path D2D leads to satisfaction, in: A World of Wireless, Mobile and Multimedia Networks (WoWMoM), 2017 IEEE 18th International Symposium on, IEEE, 2017, pp. 1–7.

[2] Y. Cai, Z. Qin, F. Cui, G. Y. Li, J. A. McCann, Modulation and multiple access for 5G networks, IEEE Communications Surveys & Tutorials 20 (1) (2018) 629–646.

[3] Y. Wu, L. P. Qian, J. Zheng, H. Zhou, X. S. Shen, Green-oriented traffic offloading through dual connectivity in future heterogeneous small cell networks, IEEE Communications Magazine 56 (5) (2018) 140–147.

[4] K. Hammad, A. Moubayed, S. L. Primak, A. Shami, QoS-aware energy and jitter-efficient downlink predictive scheduler for heterogeneous traffic LTE networks, IEEE Transactions on Mobile Computing 17 (6) (2018) 1411–1428.

[5] H.-H. Cho, C.-F. Lai, T. K. Shih, H.-C. Chao, Integration of SDR and SDN for 5G, IEEE Access 2 (2014) 1196–1204.

[6] X. Lin, J. G. Andrews, A. Ghosh, R. Ratasuk, An overview of 3GPP device-to-device proximity services, IEEE Communications Magazine 52 (4) (2014) 40–48.

[7] 3GPP, LTE Device to Device Proximity Services; User Equipment (UE) radio transmission and reception, Technical Report (TR) 36.877, 3rd Generation Partnership Project (3GPP), version 12.0.0 (03 2015).
URL https://portal.3gpp.org/desktopmodules/Specifications/SpecificationDetails.aspx?specificationId=2576

[8] WiFi Direct Alliance, http://www.wi-fi.org/discover-wi-fi/wi-fi-direct.

[9] Google Nearby API, https://developers.google.com/nearby/.

[10] A. Asadi, V. Mancuso, WiFi Direct and LTE D2D in action, in: Wireless Days (WD), 2013 IFIP, IEEE, 2013, pp. 1–8.

[11] A. Asadi, V. Mancuso, R. Gupta, An SDR-based experimental study of outband D2D communications, in: INFOCOM 2016-The 35th Annual IEEE International Conference on Computer Communications, IEEE, IEEE, 2016, pp. 1–9.

[12] A. Asadi, V. Mancuso, R. Gupta, DORE: an experimental framework to enable outband D2D relay in cellular networks, IEEE/ACM Transactions on Networking 25 (5) (2017) 2930–2943.

[13] C.-C. Tseng, J.-Y. Shih, Two-stage coalition formation and radio resource allocation with nash bargaining solution for inband underlaid D2D communications in 5G networks, Journal of Network and Computer Applications 111 (2018) 64–76.

[14] C. T. Garrocho, M. J. da Silva, R. A. Oliveira, D2D pervasive communication system with out-of-band control autonomous to 5G networks, Wireless Networks (2018) 1–14.

[15] W. Cao, G. Feng, S. Qin, M. Yan, Cellular offloading in heterogeneous mobile networks with D2D communication assistance, IEEE Transactions on Vehicular Technology 66 (5) (2017) 4245–4255.

[16] S. Cicalò, V. Tralli, QoS-aware Admission Control and Resource Allocation for D2D Communications Underlaying Cellular Networks, IEEE Transactions on Wireless Communications.

[17] B. Ma, H. Shah-Mansouri, V. W. Wong, Full-duplex Relaying for D2D Communication in mmWave based 5G Networks, IEEE Transactions on Wireless Communications.

[18] A. Asadi, Q. Wang, V. Mancuso, A survey on device-to-device communication in cellular networks, IEEE Communications Surveys & Tutorials 16 (4) (2014) 1801–1819.

[19] A. Asadi, V. Mancuso, P. Jacko, Floating band D2D: exploring and exploiting the potentials of adaptive D2D-enabled networks, in: World of Wireless, Mobile and Multimedia Networks (WoWMoM), 2015 IEEE 16th International Symposium on a, IEEE, 2015, pp. 1–9.

[20] Y. Zhang, C.-Y. Wang, H.-Y. Wei, Incentive Compatible Overlay D2D System: A Group-Based Framework without CQI Feedback, IEEE Transactions on Mobile Computing.

[21] Y. Li, M. C. Gursoy, S. Velipasalar, J. Tang, Joint mode selection and resource allocation for D2D communications via vertex coloring, arXiv preprint arXiv:1708.00872.

[22] E. Datsika, A. Antonopoulos, N. Zorba, C. Verikoukis, Cross-network performance analysis of network coding aided cooperative outband D2D communications, IEEE Transactions on Wireless Communications 16 (5) (2017) 3176–3188.

[23] A. Abrardo, G. Fodor, B. Tola, Network coding schemes for D2D communications based relaying for cellular coverage extension, Transactions on Emerging Telecommunications Technologies.

[24] 3GPP, Technical Specification Group Services and System Aspects; Policy and charging control architecture (Release 13), Technical Report (TR) 23.203, 3rd Generation Partnership Project (3GPP), version 13.4.0 (2015).

[25] S. Wen, X. Zhu, X. Zhang, D. Yang, QoS-aware mode selection and resource allocation scheme for device-to-device (D2D) communication in cellular networks, in: 2013 IEEE International Conference on Communications Workshops (ICC), IEEE, 2013, pp. 101–105.

[26] S. Maghsudi, D. Niyato, On transmission mode selection in D2D-enhanced small cell networks, IEEE Wireless Communications Letters 6 (5) (2017) 618–621.

[27] F. H. Khan, Y.-J. Choi, S. Bahk, Opportunistic mode selection and RB assignment for D2D underlay operation in LTE networks, in: Vehicular Technology Conference (VTC Spring), 2014 IEEE 79th, IEEE, 2014, pp. 1–5.

[28] D. Della Penda, L. Fu, M. Johansson, Mode selection for energy efficient D2D communications in dynamic TDD systems, in: 2015 IEEE International Conference on Communications (ICC), IEEE, 2015, pp. 5404–5409.

[29] A. Asadi, V. Mancuso, Network-assisted outband D2D-clustering in 5G cellular networks: theory and practice, IEEE Transactions on Mobile Computing 16 (8) (2017) 2246–2259.

[30] R. He, Z. Zhong, B. Ai, L. Xiong, J. Ding, The effect of reference distance on path loss prediction based on the measurements in high-speed railway viaduct scenarios, in: Communications and Networking in China (CHINACOM), 2011 6th International ICST Conference on, IEEE, 2011, pp. 1201–1205.

[31] J. S. Seybold, Introduction to RF propagation, John Wiley & Sons, 2005.

[32] J. M. Lucas, M. S. Saccucci, Exponentially weighted moving average control schemes: properties and enhancements, Technometrics 32 (1) (1990) 1–12.

[33] Y. Censor, Pareto optimality in multiobjective problems, Applied Mathematics and Optimization 4 (1) (1977) 41–59.

[34] A. Asadi, Opportunistic cellular communications with clusters of dual-radio mobiles, Ph.D. thesis, Universidad Carlos III de Madrid, Spain (2012).

[35] W. Sun, Y.-X. Yuan, Optimization theory and methods: nonlinear programming, Vol. 1, Springer Science & Business Media, 2006.

[36] A. H. Land, A. G. Doig, An automatic method of solving discrete programming problems, Econometrica: Journal of the Econometric Society (1960) 497–520.

[37] M. Belleschi, G. Fodor, A. Abrardo, Performance analysis of a distributed resource allocation scheme for D2D communications, in: 2011 ieee globecom workshops (gc wkshps), IEEE, 2011, pp. 358–362.

[38] R. Liu, G. Yu, F. Qu, Z. Zhang, Device-to-device communications in unlicensed spectrum: Mode selection and resource allocation, IEEE Access 4 (2016) 4720–4729.

[39] G. Wunder, M. Kasparick, S. ten Brink, F. Schaich, T. Wild, I. Gaspar, E. Ohlmer, S. Krone, N. Michailow, A. Navarro, et al., 5GNOW: Challenging the LTE design paradigms of orthogonality and synchronicity, in: Vehicular Technology Conference (VTC Spring), 2013 IEEE 77th, IEEE, 2013, pp. 1–5.

[40] M. Grant, S. Boyd, CVX: Matlab software for disciplined convex programming, version 2.1, `http://cvxr.com/cvx` (Mar. 2014).

[41] M. Grant, S. Boyd, Graph implementations for nonsmooth convex programs, in: V. Blondel, S. Boyd, H. Kimura (Eds.), Recent Advances in Learning and Control, Lecture Notes in Control and Information Sciences, Springer-Verlag Limited, 2008, pp. 95–110, `http://stanford.edu/~boyd/graph_dcp.html`.

[42] R. K. Jain, D.-M. W. Chiu, W. R. Hawe, A Quantitative Measure of Fairness and Discrimination, Eastern Research Laboratory, Digital Equipment Corporation, Hudson, MA, 1984.

Appendix A. DEMA vs. EMA

In order to average satisfaction values over time with no bias on new arrivals and short-lived flows, we have derived DEMA with no intention to resemble EMA. However, note that EMA corresponds to the following recurrence:

$$F_n^{EMA}(j+1) = (1-\alpha)F_n^{EMA}(j) + \alpha f_n(j), \quad \alpha \in [0,1], \tag{A.1}$$

which is similar to the DEMA scheme in Eq. (8), although the factor α is constant. Having a constant factor α has a key impact on the behavior of the EMA scheme, and provides substantial differences with DEMA. Indeed, the EMA

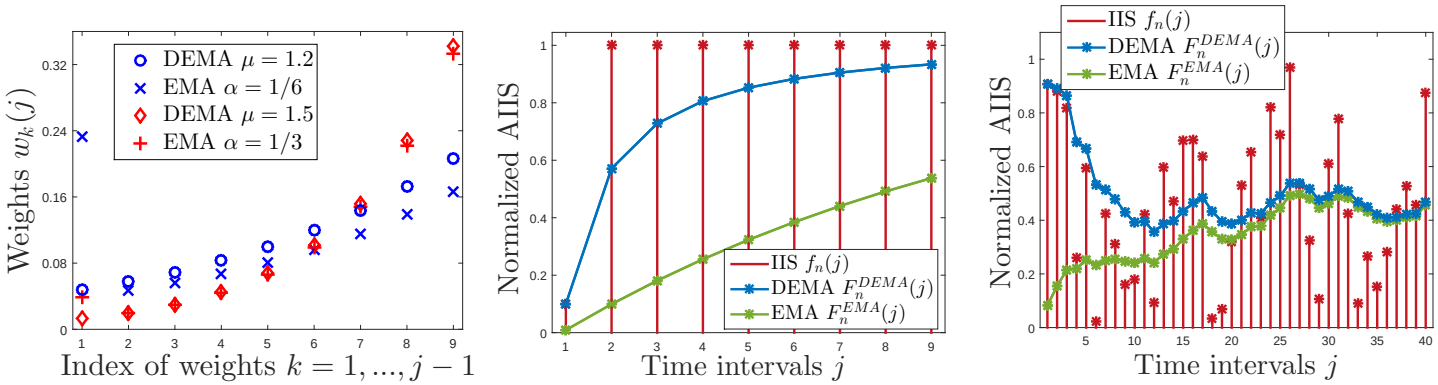

(a) Weights of DEMA and EMA schemes.

(b) Comparison of DEMA and EMA schemes in short-term history, with μ=1.5, α=1/3.

(c) Convergence of DEMA and EMA schemes in long-term history, with μ=1.5, α=1/3.

Figure A.7: Performance of DEMA in comparison with EMA.

scheme does not update properly the AIIS values $F_n^{EMA}(j+1)$ because at each new time slot $j+1$, IIS $f_n(j)$ has the same relevance (α), regardless how long the n-th flow has lived in the network. We provide more details in what follows.

Note that using EMA corresponds also to apply a weighted average of the filtered IIS values $\{f_n(k)\}_{k=1}^{j-1}$. The EMA weights, namely $w_k^{EMA}(j)$, are the following:

$$\begin{cases} w_1^{EMA}(j) = (1-\alpha)^{j-2}, & \text{if } k = 1; \\ w_k^{EMA}(j) = \alpha(1-\alpha)^{j-k-1}, & \forall 2 \leq k < j. \end{cases} \tag{A.2}$$

The weights of the EMA scheme do not follow an increasing recurrence, neither are exponentially distributed. Conversely, for DEMA we have conveniently derived increasing exponential-shaped weights (see Eq. (7)) that yield a dynamic scheme that adapts to the length of the time history—depending on j—following a one-stem recurrence (see Eq. (8)). Although the weights of EMA, $\{w_k^{EMA}(k)\}_{k=2}^{j-1}$, seem to follow also an exponential-shaped curve, the first weight $w_1^{EMA}(j)$ is out of such curve (see Figure A.7a). Such fact has a deep relevance into the performance of the satisfaction metric under the EMA scheme, as we describe below with the help of an example.

Figure A.7a shows an example of the distribution of the weights of the average filtering of IIS values for both DEMA and EMA using $\mu = 1.2$ and $\mu = 1.5$, and with $\alpha = 1/6$ and $\alpha = 1/3$. While the DEMA weights follow a pure (increasing) exponential curve—since DEMA has been designed with such purpose—we observe that EMA assigns an unnecessarily high value to the first weight, the one corresponding to IIS $f_n(1)$. Such fact goes against the principles of the desired satisfaction metric. The satisfaction metric is intended to gather the aggregate satisfaction of a flow over time by means of assigning much more relevance to the recently past IIS values. Thus, such first weight assignment disrupts the purpose of a satisfaction metric based on EMA. The issue with EMA comes from the fact that the first weight $w_1^{EMA}(j)$ has a different expression with respect to other weights as shown in Eq. (A.2). Specifically, $w_1^{EMA}(j)$ does not include the α<1 factor of the other weights, and so it gives more importance to the oldest time slot. Moreover, besides α, the weights in EMA only depend on the distance $j-k$, i.e., the time shift with respect to the current slot. As such, the weights are not adapted to the lifespan of a flow. This would not be an issue with long flows, for which the first EMA weight is practically not biased due to the fact that $\lim_{j\to+\infty} w_1^{EMA}(j) = 0$. However, current cellular

networks are extremely dynamic and mobile. Thus, the lifespan of a flow may be short or long—i.e., j may remain small or become large—so distinct flows might experience distinct and variable satisfaction levels during their lifespans in the cell, and thus the satisfaction metric should be flexible enough to account for lifespan. Also, new flows join the cell over time, so that the first period of a flow in the network receives also an unfair treatment from an approach based on EMA. This issue is not present in the design of DEMA, as shown analytically in Eq. (7) and illustrated in Figure A.7a.

As a consequence, DEMA reacts much better to changes in the individual satisfaction pattern of flows, as shown in Figure A.7b. Here, we show a simple yet very illustrative example of the behavior of DEMA in comparison to EMA. We have used an artificial set of IIS values for one flow experiencing an abrupt change of instantaneous satisfaction from 0.1 to 1 at slot j=2. Values used in the example are normalized to one for ease of readability. In Figure A.7b, the analyzed flow has received few resources in the first time slot ($j = 1$), so the first IIS value is quite low ($f_n(1) = 0.1$). From the second time slot on ($2 \leq j \leq 9$), the flow finds better signal conditions and receives much more resources, and keeps a constant satisfaction of $f_n(j) = 1$ over the rest of the time. We show the AIIS values $\{F_n(j)\}_{j=2}^{10}$ according to the DEMA (blue in the figure) and the EMA (green) schemes. Here we note that the DEMA scheme immediately reacts to the drastic satisfaction change and increases the accumulated satisfaction $F_n(j)$ over time very fast, according to the IIS values. Thus, DEMA quickly approaches the constant IIS in few time slots. Conversely, the EMA approach shows an undesired behavior in which the AIIS values provided by EMA scheme increase at a much slower rate. Indeed, the EMA approach does not react properly to the drastic IIS change. Observe that after 9 time slots, out of which the last 8 have provided a satisfaction of 1, we expect an AIIS value approaching 1. While DEMA reflects such a behavior, EMA remains approximately 50% far from the desired indicator value.

Finally, in Figure A.7c we show an example similar to the one of Figure A.7b. Here, we provide a longer and more dynamic example of (artificial/illustrative) IIS values $\{f_n(j)\}_{j=1}^{40}$ for one flow (again normalized to one). Here, the channel conditions for the analyzed flow are very dynamic, and flow service opportunities vary over time depending on new D2D discoveries, better eNB coverage, or less interference. Again, the DEMA scheme reacts quicker and more efficiently to the high dynamics of the network, while EMA scheme provides from the first time slot satisfaction values that do not adjust to the network dynamism. While the first three flow IIS values ($j \in \{1, 2, 3\}$) are above 0.8 ($f_n(j) > 0.8$), the EMA scheme averages an accumulated satisfaction of $F_n^{EMA}(4) = 0.22$. This fact reveals how undesired and unfair the EMA scheme is in dynamic D2D networks. Here we also show that the AIIS values provided by DEMA and EMA converge to the same value in long-term history, as the time approaches to infinity. This shows again the importance of DEMA scheme for flows with a short lifespan in the network, and for those who have recently joined the network. Thus, while EMA scheme may be appropriate for flows that stay forever in the cell (which is not realistic), the best candidate for highly mobile and dynamic networks is DEMA. We prove such convergence in Lemma 1.

Lemma 1. *Let $\alpha \in]0, 1[$ and let $\mu := \frac{1}{1-\alpha} > 1$. The asymptotic behavior of EMA and DEMA weights is the same, i.e.,*

$$\lim_{j \to \infty} \left| w_k^{DEMA}(j) - w_k^{EMA}(j) \right| = 0, \quad \forall k \geq 1. \tag{A.3}$$

Proof. Let $j \in \mathbb{N}$ be fixed and let $2 \leq k < j$. Since $\mu = \frac{1}{1-\alpha}$, we have:

$$\begin{aligned} \left|w_k^{DEMA}(j) - w_k^{EMA}(j)\right| = \\ \left|\frac{\frac{1}{1-\alpha} - 1}{1-(1-\alpha)^{j-1}} \cdot (1-\alpha)^{j-k} - \alpha(1-\alpha)^{j-k-1}\right| = \\ \left|\frac{\alpha}{1-(1-\alpha)^{j-1}}(1-\alpha)^{j-k-1} - \alpha(1-\alpha)^{j-k-1}\right| = \\ \alpha(1-\alpha)^{j-k-1}\left|\frac{1}{1-(1-\alpha)^{j-1}} - 1\right|. \end{aligned}$$

Since for all $j \in \mathbb{N}$ and for all $2 \leq k < j$ we have that $\alpha(1-\alpha)^{j-k-1}$ is bounded, and it is clear that $\lim_{j\to\infty}\left|\frac{1}{1-(1-\alpha)^{j-1}} - 1\right| = 0$, we finally have that:

$$\lim_{j\to\infty}\left|w_k^{DEMA}(j) - w_k^{EMA}(j)\right| = 0.$$

Now, let $k = 1$. We have that:

$$\begin{aligned} w_1^{DEMA}(j) &= \frac{\mu - 1}{\mu^{j-1} - 1}; \\ w_1^{EMA}(j) &= (1-\alpha)^{j-1}. \end{aligned}$$

Since $\mu > 1$ and $\alpha \in]0, 1[$, we have that:

$$\lim_{j\to+\infty} w_1^{DEMA}(j) = \lim_{j\to+\infty} w_1^{EMA}(j) = 0.$$

Thus, the claim follows.

□

Lemma 1 shows the relation between the DEMA parameter μ, and the EMA parameter α. Thus, in order to provide a fair comparison between both schemes, the equation $\mu = \frac{1}{1-\alpha}$ must be satisfied (note that we have properly selected the parameters used in the examples of Figure A.7 according to Lemma 1).

Appendix B. From Non-Linear Optimization to MILP

The MPD2D optimization program derived in section 4.3 is non-linear because it has one minimum-like constraint and quadratic constraints. Both cases can be linearised by standard methods, as described in what follows.

Given a user $n \in \mathcal{N}$, the constraint:

$$Y_n^3 = \min\left(1, \sum_{m \,|\, (n,m)\in\mathcal{L}} Y_{n,m}^3 + \sum_{m \,|\, (m,n)\in\mathcal{L}} Y_{m,n}^3\right) \tag{B.1}$$

can be expressed in a linear way by means of imposing the following two constraints:

$$
\begin{aligned}
2 \cdot Y_n^3 &\geq \sum_{m \mid (n,m) \in \mathcal{L}} Y_{n,m}^3 + \sum_{m \mid (m,n) \in \mathcal{L}} Y_{m,n}^3; \\
2 \cdot Y_n^3 &\leq 1 + \sum_{m \mid (n,m) \in \mathcal{L}} Y_{n,m}^3 + \sum_{m \mid (m,n) \in \mathcal{L}} Y_{m,n}^3;
\end{aligned} \tag{B.2}
$$

given that $Y_n^3 \in \{0, 1\}$ is a binary variable.

Clearly, constraints in Eq. (B.2) are equivalent to the minimum-like constraint in Eq. (B.1) because each of the summations can take only values 0 or 1 (according to the rest of the constraints of the optimization program). Hence, the equivalency follows.

Regarding the quadratic constraints, we have always the case in which the constraint contains the product of two binary variables: $Y_{n,m}^i$ and $Y_{n',m'}^{i'}$. In general, the product of two binary variables $x, y \in \{0, 1\}$ can be linearised by means of introducing an auxiliary binary variable $\pi \in \{0, 1\}$ and the following three linear constraints:

$$
\begin{aligned}
\pi &\leq x; \quad \pi \leq y; \\
\pi &\geq x + y - 1.
\end{aligned} \tag{B.3}
$$

Now, the binary variable π contains the value of the product of x and y, i.e., $\pi = x \cdot y$. Thus, we can replace any product of binary variables of the optimization program by an auxiliary variable that accomplishes the linear constraints of Eq. (B.3).

The transformations described in this section turn the non-linear optimization program of Section 4.3 into an MILP. Hence, we can apply efficient and fast algorithms to solve the MILP, which is less complex than the non-linear program.

Appendix C. Pareto-optimality

Given the node utility defined in Eq. (6), it is easy to observe that parameters and variables indexation and notations can be re-adjusted so to express Eq. (6) as:

$$
U_n = \sum_{i \in I} (\theta_n^i - \alpha_s E_n^i) \cdot Y_n^i + \sum_{j \in J} (\theta_n^j - \alpha_s E_n^j) \cdot Y_n^j, \tag{C.1}
$$

where I and J are sets of indices. Hence, index sets I and J can be joined in $K = I \cup J$ and we can express Eq. (C.1) as:

$$
U_n = \sum_{k \in K} (\theta_n^k - \alpha_s E_n^k) \cdot Y_n^k = \sum_{k \in K} \theta_n^k \cdot Y_n^k - \alpha_s \sum_{k \in K} E_n^k \cdot Y_n^k. \tag{C.2}
$$

Now, as the system utility accounts for the summation of all node utilities, we have that:

$$
U_{net} = \sum_{n \in \mathcal{N}^*} U_n = \sum_{n \in \mathcal{N}^*} \left(\sum_{k \in K} \theta_n^k \cdot Y_n^k - \alpha_s \sum_{k \in K} E_n^k \cdot Y_n^k \right). \tag{C.3}
$$

Again, if we re-adjust the indexation, we have that the system utility is a combination of a throughput decision variable and an energy decision variable:

$$U_{net} = \sum_{l \in L} \theta_l \cdot Y_l - \alpha_s \sum_{l \in L} E_l \cdot Y_l = \sum_{l \in L} \theta_l^Y - \alpha_s \sum_{l \in L} E_l^Y, \tag{C.4}$$

where $L = \mathcal{N}^* \cup K$, $\theta_l^Y = \theta_l \cdot Y_l$ and $E_l^Y = E_l \cdot Y_l$.

Now, denoting by $\mathbf{Y}$ the set of binary decision variables, and $\theta(\mathbf{Y})$ and $E(\mathbf{Y})$ the throughput and energy functions depending on the binary decision variables, the network utility may be expressed as:

$$U_{net} = \theta(\mathbf{Y}) - \alpha_{\mathbf{s}} \mathbf{E}(\mathbf{Y}). \tag{C.5}$$

So far we have defined the system utility (U_{net}) as a combination of a throughput function ($\theta(\mathbf{Y})$) and an energy consumption function ($E(\mathbf{Y})$). In reality, what we aim in our framework is to solve a multi-variable optimization problem in which we maximize users throughput and minimize energy consumption. Hence, we should maximize the tuple $(\theta(\mathbf{Y}), -\mathbf{E}(\mathbf{Y}))$, i.e., we need to find those binary decision variables $\mathbf{Y}$ such that $\theta(\mathbf{Y})$ cannot be increased without increasing $E(\mathbf{Y})$) and $E(\mathbf{Y})$) cannot be decreased without decreasing $\theta(\mathbf{Y})$. This is a Pareto-optimal solution [33].

As we are indeed maximizing $U_{net} = \theta(\mathbf{Y}) - \alpha_{\mathbf{s}} \mathbf{E}(\mathbf{Y})$, we need to prove that the solution $\mathbf{Y}$ found in this way is Pareto-optimal. As linear combination of the multiple functions is the common way of finding Pareto-optimal solutions (as done, e.g., in [17]), the proof of the following lemma is quite simple.

Lemma 2. *The solution found in an optimization problem with $U_{net} = \theta(\mathbf{Y}) - \alpha_{\mathbf{s}} \mathbf{E}(\mathbf{Y})$ as the utility function corresponds to the Pareto-optimal solution of the multi-objective optimization problem that aims to optimize the tuple $(\theta(\mathbf{Y}), -\mathbf{E}(\mathbf{Y}))$.*

Proof. Let $\mathbf{Y}^*$ be the optimal solution of the single-utility optimization problem. Assume, *reduction ad absurdum*, that there is an alternative solution $\widetilde{\mathbf{Y}}$ that is the Pareto-optimal solution of the multi-objective optimization problem but it is not the optimal solution of the single-objective optimization problem. Hence, we have that:

$$\begin{aligned} \theta(\widetilde{\mathbf{Y}}) &\geq \theta(\mathbf{Y}^*), \\ -E(\widetilde{\mathbf{Y}}) &\geq -\mathbf{E}(\mathbf{Y}^*), \end{aligned} \tag{C.6}$$

where at least one inequality is not an equality. Hence, $\theta(\widetilde{\mathbf{Y}}) - \alpha_{\mathbf{s}} \mathbf{E}(\widetilde{\mathbf{Y}}) > \theta(\mathbf{Y}^*) - \alpha_{\mathbf{s}} \mathbf{E}(\mathbf{Y}^*)$.

Since, $\mathbf{Y}^*$ is the optimal solution of the single-utility optimization problem, we have a contradiction and the claim follows. □